State diagrams for improving processing and storage of foods, biological materials, and pharmaceuticals (IUPAC Technical Report)*

Maria Pilar Buera[1,‡], Yrjö Roos[2], Harry Levine[3], Louise Slade[3], Horacio R. Corti[1], David S. Reid[4], Tony Auffret[5], and C. Austen Angell[6]

[1]*Facultad de Ciencias Exactas y Naturales, Universidad de Buenos Aires, Int. Cantilo s/n. Pabellón II Ciudad Universitaria, Buenos Aires, Argentina;* [2]*School of Food and Nutritional Sciences, University College, Cork, Ireland;* [3]*Food Polymer Science Consultancy (retired from Cereal Science, Kraft-Nabisco) Morris Plains, NJ 07950, USA;* [4]*Department of Food Science and Technology, University of California at Davis, 1 Shields Avenue, Davis, CA 95616-8571, USA;* [5]*taPrime Consulting, Sandwich, Kent, CT13 9JA, UK;* [6]*Department of Chemistry, Arizona State University, Tempe, AZ 85287, USA*

Abstract: Supplemented temperature/composition phase diagrams include the non-equilibrium glass-transition temperature (T_g) curve and equilibrium ice-melting and solubility curves. The inclusion of the non-equilibrium curve allows one to establish relationships with the time coordinate and, thus, with the dynamic behavior of systems, provided that the thermal history of such systems is known.

The objective of this report is to contribute to the potential applications of supplemented state diagrams for aqueous glass-formers, in order to describe the influence of water content, nature of vitrifying agents, and temperature on the physico-chemical properties of foods and biological and pharmaceutical products. These data are helpful to develop formulations, processing strategies, or storage procedures in order to optimize the stability of food ingredients and pharmaceutical formulations. Reported experimental data on phase and state transitions for several food and pharmaceutical systems were analyzed. Some methodological aspects and the effect of phase and state transitions on the main potential chemical reactions that can alter those systems during processing and/or storage are discussed.

Keywords: biomolecules; glass transition; IUPAC Physical and Biophysical Chemistry Division; phase/state diagrams; reaction rates.

CONTENTS

---

1. INTRODUCTION

Many components of foods, pharmaceuticals, and preserved biological materials do not exist in a thermodynamically stable condition. Thus, the conservation of their desirable properties is governed by kinetic constraints, often by their maintenance in an amorphous state. The removal of water, either by drying or freezing, induces a supersaturation of aqueous systems, leading to an increase in the cohesive forces between molecules and to constraint in the restriction of their mobility. The implications of glass formation and glass transitions in food technology have been extensively analyzed since the pioneering work by Slade and Levine in the 1980s [1–22], based on a polymer science approach. Subsequent advances in the area of preservation mechanisms of living organisms under extreme conditions, and in the conservation of therapeutic proteins [23] promoted the study of sugar and polyol properties in relation to their protective effects on labile biomolecules [24–28]. Fundamental research was then focused on dynamic aspects, related to the glass-forming properties of sugars and biopolymers, and on molec-

ular interactions that polyhydroxy compounds are able to undergo. Supplemented temperature/composition phase diagrams have been demonstrated to be helpful in determining the feasibility of occurrence of phase/state transitions [1–11]. These diagrams include the non-equilibrium glass-transition temperature (T_g) and equilibrium ice-melting and solubility curves. The inclusion of the non-equilibrium curve allows one to establish relationships with the time coordinate and, thus, with the dynamic behavior of systems, if the previous state of the sample is known.

In the first part of our report [29], the basic principles for determining the main curves that define supplemented phase diagrams were described. The objective of this second part is to contribute to the potential applications of supplemented state diagrams for aqueous glass-formers, in order to describe the influence of water content, nature of vitrifying agents, and temperature on the physico-chemical properties of foods and biological and pharmaceutical products.

2. PHASE DIAGRAMS AND PROCESSING TECHNOLOGIES

2.1 Supplemented phase diagrams

As described previously [10,14,17–22,29] in supplemented phase diagrams, the curves corresponding to equilibrium conditions (ice-melting and solubility curves) and T_g of a system are plotted as a function of the solid mass fraction, w_2, as shown in Fig. 1, being the mass fraction of water $w_1 = (1 - w_2)$ at each point. Since the different curves in Fig. 1 delimit regions where the main dynamic changes could happen as a consequence of phase/state changes [10], by applying this kind of diagram, it can be predicted whether a system is under thermodynamic or kinetic control, for given composition-temperature conditions, providing the thermal history of the sample is known [8,10,14]. The events defined by the
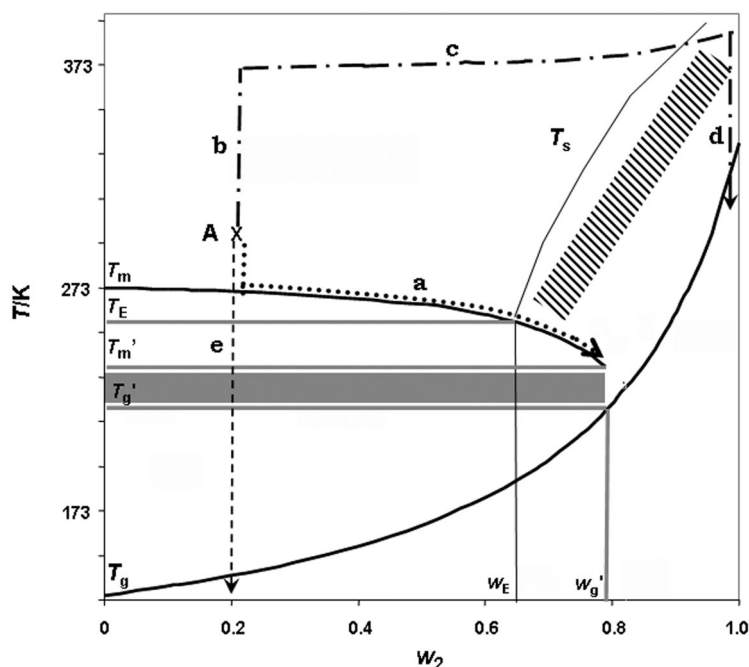

Fig. 1 Supplemented phase/state diagram showing the formation of a glass of low water content by cryoconcentration (line a) [2]; dehydration (lines b → c → d) [2] and vitrification (line e) of a system of high water content [2]. �███ Conditions for maximum rate of ice formation; ▨ conditions for maximum rate of solute crystallization.

thermodynamic curves are independent of the previous thermal history of a sample. The inclusion of the T_g curve (corresponding to a non-equilibrium transition) in supplemented state diagrams allows one to include the concept of time in which a certain event will take place or what changes will be kinetically delayed/inhibited under certain conditions. Particularly, several mathematical approaches (discussed, in Section 5.4) were established in order to predict the kinetics of specific phenomena in systems at conditions lying between the equilibrium curves and the non-equilibrium line. Reid [30] provided a very conceptual description of such a state diagram in relation to the thermodynamic phase diagram. Upon cooling of a solution of composition **A** (Fig. 1), due to supercooling (see Section 2.2) and to freezing-point depression caused by the solute, water starts to crystallize below the equilibrium temperature for ice melting (273.15 K at sea level). In a simple binary system such as that shown in Fig. 1, the point (T_E, w_E) represents the eutectic point, the temperature T_E at which, in a mixture of composition $w_2 = w_E$, both ice and solute will crystallize in a ratio that is the same as their ratio in the solution phase. This behavior is easily detectable with solutes such as $Na_2HPO_4 \cdot 12H_2O$, Na_2SO_4, Na_2CO_3, KCl, urea[1], and $(NH_4)_2SO_4$ [31].

When the solute does not crystallize under the experimental conditions, cooling the solution to below T_E will result in further ice separation, and freezing-point depression due to solute concentration will continue, but not at equilibrium. At some point, a temperature (T_m' in Fig. 1) and solute concentration ($w_2 = w_g'$) are reached, at which the viscosity of the concentrated unfrozen phase becomes a limiting factor for additional ice formation [8,12,15,20,32–34]. Thus, line a in Fig. 1 indicates a hypothetical route for a system submitted to cryoconcentration, reaching the maximum mass fraction of solids that can be achieved by freezing. At the T_g of the maximally freeze-concentrated matrix (T_g'), a glass is formed (Fig. 1) [1–11]. The point (T_g', w_g') depends on the material composition, but not on the initial solids fraction (before freezing). At a temperature below the T_g', the amorphous unfrozen phase vitrifies and exists as a glassy solid separate from the ice crystals [22].

As defined in the first part of this report [29], T_m' identifies the point and temperature at which ice formation ceases. Since it lies on the equilibrium melting curve, it is a well-defined point. T_g', however, being related to a non-equilibrium process, can have many temperature values depending on how it is measured (whether the onset or some other value over a range of temperatures is used, and depending on scanning rate or frequency employed in the measurement—see Section 5.1).

Any system that is not at its highest cryoconcentration level will show a T_g value lower than that representing maximum freeze-concentration because it retains more unfrozen water.

No further unfrozen water is able to crystallize below T_g', and therefore, depending on viscosity in the vicinity of T_g', the ice melts at the same temperature as it was formed. Hence, the theoretical values for T_g' and T_m' are the same. However, partial softening of the glass is required before time-dependent ice formation can occur. This is shown by maximally freeze-concentrated solutions of most sugars, which often exhibit onset of melting above T_g' and in some cases above the endpoint temperature of the glass-transition range. At a given extent of freeze-concentration, the melting temperature of ice and the T_g theoretically reach the same temperature (T_g' for T_g or T_m' for T_m) [22].

Solute properties and solute–water interactions affect the amount of water that remains unfrozen in the matrix and thus the temperature range at which any process involving ice formation should be performed. These variables should be taken into account in the design of processes and frozen-system formulations. Table 1 shows the T_E and T_g' values of some selected inorganic salts. It has to be noted that the different kinetics that govern solute and water crystallization make ice crystallization and cryoconcentration possible beyond the conditions corresponding to the eutectic point (compare solute concentration at the points w_E and w_g' in Fig. 1, and the values of T_E and T_g' in Table 1).

---

[1]diaminomethanal

Table 1 Reported values for the glass-transition temperature of the maximally freeze-concentrated matrix (T_g') and for the eutectic point (T_E) of some inorganic salts.

Salt	T_e/K	T_g'/K	Reference
KCl	262	–	31
$(NH_4)_2SO_4$	254	–	31
$Na_2HPO_4 \cdot 12H_2O$	272	–	249
NaH_2PO_4	272.5	228	249
		208	250
KH_2PO_4	–	218	250
Na_2SO_4	271	–	31
Na_2CO_3	270		31
NaCl	251	<213	31, 251
$K_2HPO_4 \cdot 6H_2O$	259	192	249
$NaHCO_3$	269	–52	44
$CaCl_2$	221	–95	31
$MgCl_2$	162	–	31

2.2 The freezing process: Ice crystallization and the cryoconcentrated matrix

Freezing is a process of ice crystallization from supercooled water. A supercooled system is that in which no crystallization has occurred, even if it is below the ice-melting (liquidus) or solubility (solidus) curves (Fig. 1). In the case of water, it should undergo a stage of ice nucleation, followed by the growth of ice. Nucleation can be regarded as a kinetic process for ice nuclei to overcome a kinetic barrier, the so-called nucleation barrier, under a given thermodynamic driving force, which is proportional to the supercooling. Although ice growth is thermodynamically favored at temperatures below 273.15 K, ice nucleation is not kinetically favored in pure water, which can remain liquid down to nearly 233 K, the homogeneous nucleation temperature (T_h), if free of ice-nucleating species.

The degree of supercooling (SC) is the thermodynamic impulsive force for crystallization, and it is defined as

$$SC = T_m - T \tag{1}$$

where T is the actual (subfreezing) temperature and T_m is the equilibrium melting point of ice for a given w_2.

Supercooling is limited by heterogeneous nucleation in the presence of solid impurities. Almost all organic and inorganic solids can catalyze ice formation (i.e., serve as heterogeneous ice nucleators) at temperatures between 258 and 233 K. Certain compounds can serve as nuclei at temperatures as high as 267 K, and a wide variety of impurities make homogeneous nucleation impossible. Ice nucleation at temperatures above T_h is induced by heterogeneous ice nucleating agents (INAs) [35]. Ice nucleation preferentially occurs on these impurities (dust, mold spores, etc.), since they lower the energy required to form the interface between the existing phase and the new phase.

The transient ice-like embryos formed by aggregation of water molecules are subjected to continuous fluctuation in size due to the incorporation of new molecules and the detachment of others. For a given temperature, there will be a critical radius that defines the minimum size a nucleus can have to be a stable crystal, and this critical radius decreases with decreasing temperature below T_m. Thus, the rate of nucleation would increase with decreasing temperature below T_m. However, this effect is limited by the decrease in molecular mobility with increasing viscosity as temperature decreases [36]. As a result of the opposite effects that influence the increase in the extent of supercooling (either by
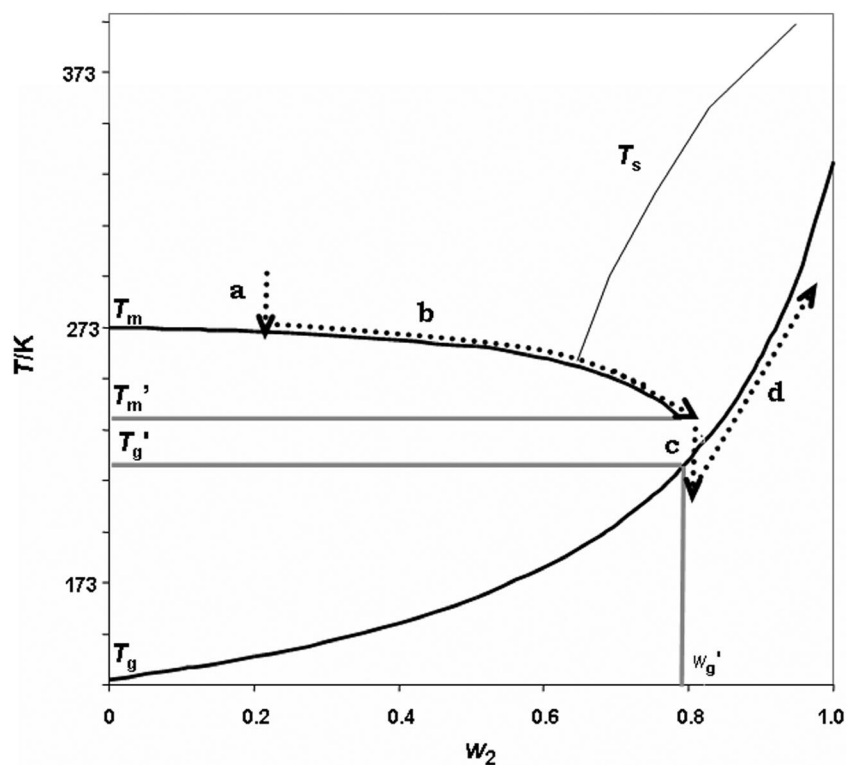
Fig. 2 Supplemented phase/state diagram showing the formation of a glass of low water content by lyophillization (through lines a → b → c → d) (modified from [2]).

decreasing temperature or by increasing T_m), the overall crystallization rate is maximum at some intermediate temperature values lying between T_m and T_g [2].

Because the Gibbs energy barrier for three-dimensional nucleation of water is much higher than that for ice crystal growth, ice crystal growth becomes in most cases much easier than nucleation; once ice nuclei are formed, the rapid growth rate leads to instant freezing [37]. In order to avoid water crystallization, the cooling rate should thus be very high. Due to their more complex structure, solute crystallization is generally slower than that of ice, and this is the basis of cryoconcentration protocols: solute crystallization is delayed, while water crystallization continues, beyond the eutectic point, up to the point where kinetic restrictions operate [2].

Freezing and melting of water are important to such food processes as freeze-concentration, freeze-drying, and freezing. The combined effects of decreasing temperature and increasing concentration impose restrictions on the molecular mobility of a system. The state of the unfrozen matrix markedly affects the stability of a frozen product.

Crystallization and recrystallization of ice and other compounds in partially freeze-concentrated solutions affect the quality of frozen foods. These processes are also related to the glass transition and dilution of freeze-concentrated systems [20–22,38]. Reid et al. [39] discussed the role of the glassy state in the stability of frozen products, and they described methods for identifying the temperature at which the glassy state is entered and the composition of the glassy phase, analyzing the differences in the results obtained from the application of different methods. The mechanisms of freezing are also to be considered, since they affect the final composition of the unfrozen matrix [40].

During heating of frozen binary solutions of sugars and water, a glass transition of the freeze-concentrated matrix, at T_g, and ice melting, at T_m, can be detected. A partially freeze-concentrated matrix

(as that obtained for rapidly frozen materials) may also show ice crystallization during rewarming at a given temperature above T_g. Such ice crystallization is an exothermal event often referred to as devitrification. Isothermal holding at a certain temperature below the onset temperature of ice melting at T_m' of the maximally freeze-concentrated system, but above T_g', (shown in Fig. 1 as a shaded area) allows time-dependent ice formation. For the same reason, thermal treatments or annealing are often applied to achieve maximum ice formation.

Below T_m' the viscosity of frozen materials increases until a glass is formed at T_g'. At temperatures below T_m', if the maximum amount of ice has formed, various frozen foods should exhibit improved stability [2,4–6]. At T_m' the mobility of the matrix is sufficient to allow for dilution by liquid water in the experimental time scale, so the enthalpy of melting starts to be observed. Hence, until T_m' is reached on warming, there is no dilution of the matrix, and the concentration at T_g' and at T_m' is the same.

2.3 Glass formation: Drying and vitrification

Amorphous glasses are formed by a continuous process in which no interface or solidification front is involved. Glass structure is comparable to that of a liquid (some short-range order is observed, but no long-range order), but its properties are similar to those of a solid. Amorphous glasses are in a non-equilibrium state, since these systems are located below the saturation curve, in the temperature-composition state diagram (Fig. 1), where the thermodynamical stable form is the crystal. However, in the glassy state, most structural changes occur very slowly and only small motions of molecules, mainly rotational motions of side chains and vibrations, may occur [2,8]. The stabilizing effect of glasses is due to the formation of a matrix that strongly inhibits diffusion and molecular mobility (vitrification), kinetically delaying physical changes and chemical reactions in most cases. Thus, crystallization of the amorphous solid is kinetically delayed if the sample remains in the glassy state, below T_g. Most physical changes (including solute crystallization) result from the sharp increase in molecular mobility that occurs above their T_g [2,8,14–16]. As shown in Fig. 1, the T_g of a material is a function of the relative proportion of its glass-forming components and water. As depicted in Fig. 1, in order to form a glass from a system starting at room temperature, two simple routes can be followed. One route involves heating up to above the boiling point of water (line b), rapid dehydration (line c), and rapid cooling down (line d) [2]. The main requirement is to pass through the regions of solute or ice crystallization (marked in Fig. 1) adequately fast.

Typical products containing glassy components of low water content are dehydrated foods, ingredients and tissues, and pharmaceuticals powders (freeze- or spray-dried).

The alternative, second route is to form a glass at high water content, avoiding ice crystallization by rapid cooling into the glassy state, or vitrification (line e [2] in Fig. 1). At present, long-term storage of living cells is performed by vitrification of whole cells or tissues under liquid nitrogen (at 77 K). Vitrification of high-water-content systems, as a cryopreservation method, has many primary benefits, such as the avoidance of ice crystal formation through increased speed of temperature conduction, which provides a significant increase in cooling rates. This can eliminate structural damage of the material during freezing, but mass-transfer rates limit the sample size in which this can be achieved and thawing is never rapid enough to prevent crystallization from causing extensive damage during rewarming [41]. It is to be noted that the maximum rate of ice nucleation occurs just above T_g, and the maximum ice-crystal-growth rate occurs just below T_m (Fig. 1). Thus, the many nuclei formed during cooling can cause massive ice growth during rewarming. This leads to devitrification. The main concern on cooling is the maximum nucleation range near T_g. The most common current uses of vitrification are for biological embryo and tissue preservation [42].

For the conservation of tissues or other biological structures, the addition of a cryoprotectant may allow cooling down to the region of T_g without formation of ice crystals, if cooling is fast enough. If

nuclei are formed, the rapid cooling and high viscosity near T_g in the presence of cryoprotectant will not allow the nuclei to grow very much and thus prevents them from being detrimental. Enough cryoprotectant to depress T_m will reduce the temperature of nucleation to T_g, thereby delaying nucleation. Dissolved sugars and polymers form glasses readily once freeze-concentrated. Certain disaccharides effectively protect proteins and cell membranes against chilling, freezing, and dehydration, as will be discussed later.

2.4 Lyophilization: Freezing and drying

Lyophilization, or freeze-drying, only proceeds within narrow temperature and pressure ranges, in which a frozen product is heated without ice melting. Franks has provided several publications in which the principles, processes, and variables of freeze-drying are analyzed in detail, mainly with regard to the production of pharmaceuticals [31,43–47]. The principle of glass production by lyophilization is illustrated by the state diagram for a binary system, presented in Fig. 2. Freeze-drying involves the sublimation of ice previously formed under vacuum (primary drying). During this stage, the solids are concentrated in the nonfrozen phase, according to routes a–d [2] in Fig. 2.

Due to the very low pressure (<100 Pa) in the freeze-drier chamber and to the sublimation of water, the temperature at the ice front is very low during ice sublimation. At the very end of the primary drying, the last crystals of ice take the heat of sublimation from the nonfrozen phase, which temperature decreases, as indicated in Fig. 2. Immediately after this, the sample temperature rises asymptotically toward the shelf temperature, and this marks the end of the sublimation stage. As discussed earlier, in every system, a given amount of water remains unavoidably unfrozen. Further drying is thus needed after primary drying, in order to eliminate the water that could not be sublimated, because it remained unfrozen.

The secondary drying is performed by desorption under vacuum (hypothetically represented by line d in Fig. 2) [2]. Product formulation is one of the main variables that is controllable to produce an acceptable lyophilized product. Much of the formulation rationale of the past has been empirical, but the scientific basis for using lyophilization additives emerged in the 1990s [48]. A number of works concerning the mechanisms by which additives can affect protein stability in solution, during drying and in frozen, stored, and reconstituted systems improved the knowledge base [25,49–52], allowing the achievement of more scientifically based protocols.

During the primary drying stage of freeze-drying, the concept of T_g' is useful to explain why structural collapse does not take place below its value [8], but the variable that is useful to explain why it happens is T_m', because above this temperature, ice melting is involved in the collapse process. T_m' is critical to the occurrence of structural collapse (a phenomenon characterized by material flow and disruption of structure integrity) in various materials during freeze-drying [22]. Above T_m', increasing water content due to ice melting leads to a rapid decrease in viscosity, because of dilution of the food solids (increasing plasticization by unfrozen water). The onset of ice melting at T_m' is the primary reason for "mobility" above that point. Once T_m' is exceeded, T_g' is no longer a necessary reference state, because of ice melting and increasing plasticization of the unfrozen phase. In this sense, the glass-transition temperature referred to as T_g' and ice melting above T_m' are two different concepts, although both refer to the same maximum freeze-concentration phenomenon.

T_m' should always occur at the same concentration as T_g'. This reflects the fact that the kinetic limits for maximum ice formation depend on the solute and temperature. The glass transition does not need to be completed during heating of a material, in order to allow ice melting to start at the same temperature at which ice formation was completed during freezing (T_m'), and a system with unfrozen phase of solute concentration w_g' was formed.

The vapor pressure of ice which provides the driving force for water removal during the primary drying in freeze-drying, increases logarithmically with increasing temperature. Therefore, from a

process economic standpoint, the ice-sublimation stage profits from as high a temperature as possible [46]. Setting of the correct sublimation temperature depends on the formulation details. In practice, T_g' values above 233 K should be aimed at by judicious formulation [46]. For most products, T_g' will be governed by the nature and proportions of excipients and salts in the product. However, it should be kept in mind that sample collapse during the primary drying period will occur, if T_m' is surpassed.

    Glucose[2], fructose[3], sucrose[4], and lactose[5] are among the most important natural carbohydrates in foods. They are also important cryoprotectants in the freezing of biologically active materials. The various phenomena related to freezing and melting of these aqueous carbohydrate solutions have been studied intensively since many decades ago [33], but some of the basic phenomena have been understood more recently [2,15,22,53,54], even though there is still some discussion on the true nature of the transitions [55]. The complex thermal transitions in frozen systems are time-dependent and include both equilibrium and non-equilibrium phenomena, such as the viscosity-controlled nature of ice formation at low temperatures. Therefore, only annealing of frozen solutions at an appropriate temperature may promote maximum ice formation, which is extremely important to freeze-drying. It has been observed that, for example, flavor retention during freeze-drying is significantly improved, if the material is slowly frozen [56], and therefore allowed to form a greater amount of ice.

3. PHASE TRANSITIONS AND THE STORAGE STABILITY OF PROCESSED SYSTEMS

During product storage, many physical/chemical changes may occur in the kinetically stabilized systems [57]. These time-/temperature-dependent changes are critical in the maintenance of component functionality, as well as nutritionally important and/or determinant to the sensory acceptance of foods by consumers. The significance of state and phase transitions to the stability of amorphous food materials, and also their impact on chemical and enzymatic reactions, has been evaluated [7,10,14–18,58–64]. State transitions can also be related to food safety.

3.1 Physical changes

3.1.1 Collapse, stickiness, and caking
The effect of glass transition is clearly reflected in certain physical aspects of foods and pharmaceutical systems. White and Cakebread [65] described various physical defects in frozen and dehydrated foods stored above T_g. Caking of amorphous powders, stickiness, collapse, crystallization, and aroma loss have been described as temperature/time/water content-dependent phenomena occurring above a collapse temperature [66–69]. Acceleration of these phenomena is the result of the decreased viscosity and consequent increase in mobility, when a system transforms from the glassy (below T_g) to the rubbery (above T_g) state [8]. In the case of amorphous powders, the formation of bridges between adjacent particles, and then aggregation, was shown to take place when surface viscosity decreased because of an increase in temperature or water content, and reached a critical value (at the sticky point temperature, T_{sp}) that depended on particle size and the characteristic time scale of the method used to monitor the changes. T_{sp} and T_g were observed to be similarly affected by increasing the mass fraction of water, with T_{sp} being close to the T_g end value, i.e., about 20 K above T_g onset [2,8,15]. As resistance to flow is inversely proportional to $\Delta T = T - T_g$ caking rates can be modeled as a function of ΔT using Williams–Landel–Ferry (WLF) behavior [2] (see Section 5.4).

---

[2]See the systematic IUPAC name in Table 4.
[3]See the systematic IUPAC name in Table 4.
[4]See the systematic IUPAC name in Table 4.
[5]See the systematic IUPAC name in Table 4.

In Section 2.4, we mentioned that structural collapse can occur during freeze-drying, due to surpassing T_m' of the freeze-concentrated frozen material. Such samples would show a foamy or liquid-like appearance, depending on the extent of temperature increase above T_m'. During air-drying, or during the storage of dried products, collapse is manifested by a macroscopic reduction of the system volume (shrinkage), and is based on the same process as stickiness [8]. Water content is a critical parameter in caking of amorphous foods, through its "depressing" (plasticizing) effect on T_g [8], and it is typically controlled through proper formulation, adequate packaging, and/or anti-caking agents. Modification of T_g can be a means of reducing the caking rate [8,70,71].

While these phenomena can be responsible for the deterioration in quality of powdered products, agglomeration—an example of a controlled caking process—can be used to improve product appearance, handling, and dispersability in water. The mean apparent activation energy measured for collapse of amorphous sugar mixtures, which is in the 200 to 400 kJ mol^{-1} range) [72] indicates the large temperature dependence of the phenomenon, which is similar to that for viscosity in the temperature range above T_g (WLF behavior, see Section 5.4).

3.1.2 Crystallization of solutes

The same criteria affecting the relative rates of embryo nucleation and crystal growth, discussed with regard to ice in Section 2.2, are valid when analyzing solute crystallization, and the area corresponding to the conditions for maximum rate of solute crystallization is marked in the state diagram of Fig. 1 (shaded area below the solubility curve).

Sugar crystallization in foods has been shown to be a consequence of changes in molecular mobility occurring above T_g [13]. Crystallization of lactose impairs the solubility of dairy powders, and accelerates damaging chemical changes [73,74], although controlled crystallization can be used to reduce the hygroscopicity and caking tendency of whey powders and other dairy powders. In the temperature ranges where crystallization is mainly controlled by molecular diffusion, i.e., close to T_g, the effect of water content can be explained through its influence on T_g.

The state diagram (e.g., Figs. 1 and 2) describes two possibilities for sugar crystallization occurrence [16,17,75]:

- Cooling down a concentrate well below the solubility line. Vuataz [75] observed that about 30 K below the lactose solubility curve, spontaneous nucleation of the less-soluble lactose form (alpha monohydrate) occurs.
- Heating an amorphous sugar to above its T_g curve provokes sugar-crystal nucleation [2]. The crystallization rate is expected to be $(T - T_g)$-dependent [2,8], and the crystal structure can be affected by cosolutes [75].

3.2 Protein stability

Most proteins can lose their native functionality, due to chemical and physical changes, when stored for extended periods in aqueous solution. Protein-drug pharmaceuticals or high added-value food-protein ingredients are often freeze-dried to achieve a stable product, typically with w_1 lower than 0.1. However, depending on formulation, storage temperature, and residual water content in the protein phase, protein stability in the solid state can be worse than that in the liquid state, and appropriate excipients should be present during processing, to facilitate formation of suitable matrices [26].

3.2.1 Freezing-induced damage

Although proteins are often frozen during processing or freeze-dried after formulation, to improve their stability, they can undergo degradation leading to losses in biological activity during such processing. The main mechanisms by which proteins are affected during freezing and dried storage are unfolding, aggregation, deamidation, and oxidation [23]. The kinetics of those mechanisms change during freezing, because the physical environment of the protein changes dramatically, leading to the development

of stresses that impact protein stability. Low temperature, freeze-concentration, and ice formation are the three chief stresses that occur during cooling and freezing. Stambrini and Gabellieri [76] have shown that the presence of an ice surface promoted a structural perturbation of a protein, affecting its tertiary structure. The cryoprotectants sucrose and glycerol[6] inhibit the freezing-induced perturbations of several analyzed enzymes in frozen environments. Freeze-concentration can facilitate secondary reactions, crystallization of buffer or non-buffer components, phase separation, and redistribution of solutes. The partial precipitation of buffer salts can also promote dramatic pH changes during freezing. For example, the dibasic form of sodium phosphate crystallizes in frozen solutions, resulting in a system that contains the monobasic salt, which has a very low pH [77]. To minimize the changes caused by pH reduction upon freezing, the use of sodium phosphate should be avoided [51]. However, note that if a buffer composition consists of potassium phosphate and NaCl, sodium phosphate will be formed. The presence of other components in the formulation may prevent the crystallization of dibasic sodium phosphate. The performance of other solutes (sugars, polyols) as buffer crystallization inhibitors is difficult to assess, and specific studies should be performed under each particular experimental situation [51]. An understanding of the different kinds of stresses to which a protein is subjected under frozen conditions is critical to the determination of the probability of protein degradation during freezing, and is therefore important in the design of stabilizer systems [78].

3.2.2 Changes upon storage of glassy formulations

Changes in molecular mobility, local pH, water content, and crystallinity of excipients may affect the chemical degradation rate of freeze-dried proteins or membranes in subsequent storage.

Much knowledge about protein stability is derived from understanding how living organisms survive thermal and hydric stresses [79] (see Section 6). Besides forming glasses, in which kinetic restrictions to physico-chemical changes (such as chemical reactions and crystallization) operate, sugars achieve their ability to protect proteins and membranes by way of hydrogen-bond interactions with the active biomolecules. Sugars, and especially α,α-trehalose[7], were found to be more effective protein protectants than were biopolymers (in spite of the sugars' lower T_g values), even at relatively high temperatures [26,80]. In amorphous trehalose matrices, several enzymes retained quite good activity in the supercooled region, but their activity decreased drastically when the sugar crystallized [81,82]. When a sugar crystallizes, a protein is excluded from the sugar crystals, and is thus exposed to an environment lacking any stabilizing effect from sugar hydroxyl groups, and in which the changes in pH, concentration of reactive groups, and ionic strength may also negatively affect their stability. However, it has been observed that if sugar crystallization is inhibited or conveniently delayed, the protective action of sugars on many enzymes may be extended to the supercooled-liquid state [80,83]. Mazzobre et al. [81,83] analyzed the stability of several freeze-dried enzymes (yeast β-galactosidase[8] and invertase[9], honey amylase[10], soy urease[11], and soy transaminase[12]) over a wide range of temperature/water content conditions. Materials capable of forming amorphous matrices, but with different physico-chemical characteristics, were chosen to compare their efficiencies in protecting the enzymes. In polymeric glassy matrices, enzyme stability decreased due to either increasing water content at a given temperature or increasing storage temperature at a fixed water content. Figure 3 [96] shows the remaining activity of lactase[13] in various dehydrated polymer and sugar systems, stored for 24 h at 340 K, as a function of

---

[6]See the systematic IUPAC name in Table 4.
[7]See the systematic IUPAC name in Table 4.
[8]β-D-galactoside galactohydrolase, E.C. number 3.2.1.23
[9]β-D-fructofuranoside fructohydrolase, E.C. number 3.2.1.26
[10]4-α-D-glucan glucanohydrolase, E.C. number 3.2.1.1
[11]urea amidohydrolase, E.C. number 3.5.1.5
[12]L-aspartate:2-oxoglutarate aminotransferase, E.C. number 2.6.1.1
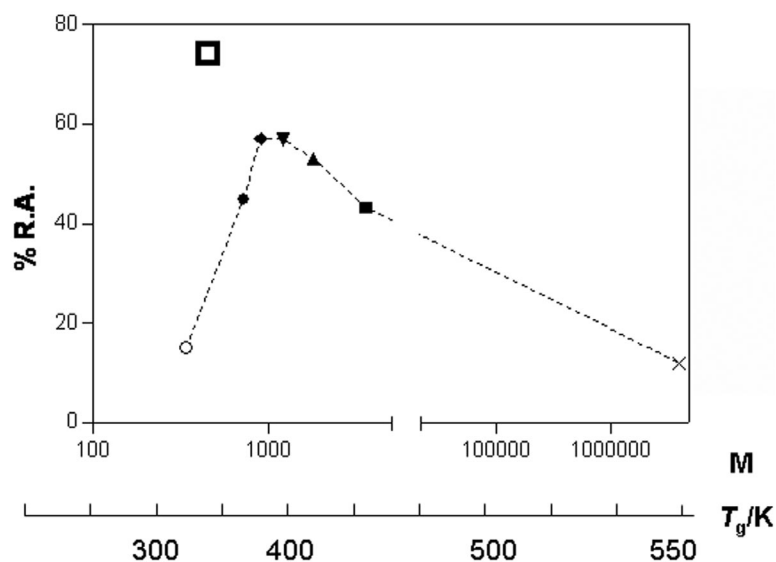[13]lactose galactohydrolase, E.C. number: 3.2.1.108

Fig. 3 Percent remaining lactase activity (% R.A.) after 24 h at 343 K in dehydrated systems, as a function of matrix T_g and molar mass (M): ○ 342 (maltose); ● 720; ◆ 900; ▼ 1200; ▲ 1800; ■ 3600; ✕ starch ; □ trehalose, from ref. [96].

T_g. The dotted line in Fig. 3 connects the enzyme's remaining activity values in amorphous matrices of maltose[14], maltodextrins[15] of different molecular weights, and native starch (all of which are oligomers or polymers of glucose). Although the T_g values for maltose, lactose, and melibiose[16] were similar to those for trehalose and raffinose, the enzyme was less protected in lactose or maltose matrices, because these reducing sugars can participate in the Maillard reaction, which can affect the active-site conformation and hence the catalytic activity of the enzyme. Other workers had also observed that maltodextrins were less effective than trehalose in protecting membranes and proteins in glassy systems [26], and this difference was attributed to a lower capacity of such polymers to form hydrogen bonds with sensitive components. Crowe et al. [26] concluded that a direct hydrogen-bond interaction between the protective agent and the protein during drying is required for stability. Another impactful property of trehalose is its degree of molecular packing. In addition to trehalose's ability to form hydrogen bonds with biomolecules [46], its low free volume enhances the packing in an amorphous matrix [84].

Lactase stability in amorphous maltose, maltodextrins, and native starch matrices was maximum in maltodextrin matrices of intermediate molar masses, as shown in Fig. 3, where the reaming enzymatic activity is plotted as a function of molar mass and T_g. The trehalose matrix is included for comparative purposes. Those intermediate molar mass matrices contained oligosaccharides that were necessary to stabilize the enzyme and had an adequate molar mass to interact with it. The large molar mass of starch, its partially crystalline structure, and its superstructural arrangement reduced the capacity of this matrix to interact with the enzyme. The stability of the enzyme in such dried matrices (Fig. 3) was not only related to supramolecular aspects (such as those determined by T_g), and to the molecular mobility of a matrix, but it was also dependent on other factors such as chemical reactivity, molar mass, and conformation or molecular structure of a given matrix.

---

[14]2-(hydroxymethyl)-6-[4,5,6-trihydroxy-2-(hydroxymethyl)oxan-3-yl]oxyox ane-3,4,5-triol

[15]Maltodextrins derive from starch and are composed by a mixture of linear oligosaccharides consisting only of $1 \rightarrow 4$ linked α-D-glucopyranosyl residues such as maltotriose, maltotetraose, etc.

[16](2R,3R,4S,5S,6R)-6-[[(2S,3R,4S,5R,6R)-3,4,5-trihydroxy-6-(hydroxymethyl)oxan-2-yl]oxymethyl]oxane-2,3,4,5-tetrol

The addition of polymers, other sugars, or salts may extend the protective effect of sugars to the supercooled region, by delaying crystallization [85–87]. In dairy systems, the presence of proteins delays lactose crystallization, in comparison to pure lactose systems [88]. Gelatin[17] inhibits raffinose[18] crystallization, and in the presence of bovin serum albumin, sucrose or raffinose crystallization is inhibited, even at high water mass fractions (84 %) [89].

A second additive such as a polymer, which would raise the overall T_g of pure sugars, would reduce molecular mobility and inhibit crystallization. According to the aspects discussed above, potential strategies to avoid sugar crystallization in low-water-content foods, ingredients, or pharmaceutical formulations could involve vitrification or delay of sugar crystallization in supercooled media, which could be achieved by combinations of biopolymers, salts, or other sugars. For example, Leinen and Labuza [90] and Belcourt and Labuza [91] were able to successfully suppress sucrose recrystallization by the addition of raffinose to a cotton candy formulation and soft cookies, respectively, which consequently improved the properties of those products.

3.2.3 Consequences of the presence of salts on the protective effect of sugars

The presence of electrolytes has a profound influence on the thermodynamical and kinetic aspects related to binary sugar–water systems. It is worth emphasizing that care should be taken, when extrapolations from data for pure sugars are employed, to predict the characteristics of complex materials containing salts. If the aim is to produce an amorphous cryoconcentrated matrix, excipients should not crystallize, but should give rise to kinetically stable solutions, which can be produced by formulations with high T_g' values. An inspection of Table 1 shows that many mineral salts may either cause eutectic precipitation or contribute to a very low system T_g'. The kinetics of ice formation (at high water contents), and of sugar crystallization from the amorphous state, are modified in the presence of salts, which over time affect the protective action of such matrices [86,92]. The main changes in a binary sugar–water system, promoted by the addition of salts, are illustrated in Fig. 4. In frozen systems, salts exert a colligative effect and promote dilution of the maximally concentrated unfrozen phase, decreasing w_g' (from w_{g1}' to w_{g2}' in Fig. 4) due to the increase of non-frozen water content. Inhibition of ice crystallization in sugar–salt–water systems is caused by colligative freezing-point depression (by lowering the T_m of the mixture), non-equilibrium freezing-point depression in the proximity of T_g', and a concomitant increase in the amount of unfrozen water in the amorphous phase. Consequently, the T_g' of this phase is depressed. A reduced enzyme activity was observed in such salt-containing systems [92].

In low-water-content systems, the presence of salts also resulted in retarded sugar crystallization, even when T_g remained unchanged [86]. Omar and Roos [205] reported that T_g for lactose was not greatly affected by the presence of salt in lactose–salt mixtures, but that salt caused dramatic changes in the water-sorption and crystallization behavior of lactose, due to differences in hydrogen bonding between water and lactose, induced by the presence of salt.

Measurements of electrical conductivity in concentrated sugar–salt–water systems [92] revealed a high degree of local inhomogeneities, which were induced by preferential solvation of the ions, as a consequence of stronger ion–water interactions, compared to ion–disaccharide interactions. Therefore, while ion mobility is enhanced by a low-viscosity local environment, it is expected that the mobility of sugar molecules would be depressed by a high local viscosity. The situation could also be described in terms of spatially heterogeneous dynamics [93], as was detected in supercooled liquids by different techniques. The dynamics in regions separated by a few nanometers could differ by several orders of

---

[17]Gelatin is a mixture of purified protein fraction obtained either by partial acid hydrolysis or alkaline partial hydrolysis of animal collagen.

[18](2R,3R,4S,5R,6R)-2-[(2S,3S,4R,5R)-3,4-dihydroxy-2,5-bis(hydroxymethyl)oxolan-2-yl]oxy-6-[[(2S,3R,4S,5S,6R)-3,4,5-trihydroxy-6-(hydroxymethyl)oxan-2-yl]oxymethyl]oxane-3,4,5-triol

Fig. 4 State diagram illustrating the effect of electrolytes on ice and sugar transitions for a sugar system. T_s: solubility curve for the sugar; T_m ice-melting curve for systems with and without salts (dotted line and plain line, respectively), and the corresponding solid mass fractions of the maximally cryoconcentrated matrices, w_{g2}' and w_{g1}'; T_g: glass-transition temperature of the sugar aqueous systems [92].

magnitude. Dramatic changes in the short-range dynamics of sugar–water systems could occur, without modifying T_g of the system, as a result of supra-structural relaxations. The effect of salts, with regard to sugar crystallization kinetics and enzyme inactivation, seems also to be connected with the magnitude of their effect in disrupting the tetrahedral hydrogen-bond network of water [83]. Water "structure-maker" ions (citrate[19] > acetate[20]; Mg^{+2}) enhance the tetrahedrally coordinated hydrogen-bond structure of water, but water "structure-breakers" ions (e.g., K^+) disrupt the tetrahedral coordination of water. Some ions, such as Na^+ or Cl^-, do not have a definite effect [94], and trehalose is suggested to act as a structure-breaker, but to provide enzyme stabilization by way of strong hydrogen-bonding interactions [95]. In restricted water environments, such as dehydrated (or frozen) systems discussed in the present work, the amount of water determines the kinetics of phase changes and of enzyme inactivation. Thus, the type of water–ion interactions is manifested in such dynamic changes, and the so-called Hofmeister series offers the potential to help in their description.

---

[19]2-hydroxypropane-1,2,3-tricarboxylate
[20]ethanoate

The effect of salts on the phase diagrams for sugars was directly related to the charge/mass ratio of the cations present (Mg > Ca > Na > K) [81,83,85,86,92,96]. The selection of appropriate sugar–salt mixtures could be valuable in the formulation of media for particular applications in which ice crystallization must be avoided.

3.3 Maillard reaction

The Maillard reaction is one of the main causes of protein modification. The reaction between reducing sugars and amino groups was first described by the physician Louis-Camille Maillard in 1912. It has been extensively studied in the food area. In a more general view, the chemistry of the Maillard reaction comprises the non-enzymatic modification of amino compounds by carbonyl-containing compounds. Thus, in addition to food science, this reaction has gained considerable importance in pharmaceutical and soil science, and also in clinical areas, since many human pathologies are derived from the in vivo non-enzymatic glycosylation of proteins [97–99]. The Maillard reaction may have positive or negative impact on the quality of food products, but it is always detrimental to pharmaceuticals or biological materials during storage. The expansion of new technologies, such as the development of natural flavors, pigments, emulsifiers, antimicrobials and antioxidants; the formulation of protective media for biological systems and ingredients; and the controlled modification of the functionality of biomolecules, makes necessary an in-depth analysis of Maillard reaction kinetics and the involved variables, in order to direct those new technologies toward desirable purposes.

The rate of the Maillard reaction is strongly dependent on the concentration, ratio, and chemical nature of the reactants, and on temperature, water content, pH, and water activity (a_w) [100], but it is also influenced by the physical state of a given medium.

In aqueous liquid systems, the Maillard reaction rate decreases continuously as a_w increases, mainly due to the fact that water is a product of the reaction [101–103]. However, in solid or very viscous systems, in which reactants are subjected to mobility restrictions, a maximum reaction rate is observed at a given intermediate a_w value. Thus, the presence of a maximum in a plot of rate vs. water mass fraction content is a consequence of the low reaction rates resulting from mobility limitations of reactants (at low water contents) and from inhibition by product (at high water contents) [61]. For the purpose of elucidating the applicability of phase/state diagrams, in order to predict the kinetics of the Maillard reaction, several systems with different structural characteristics were analyzed: highly collapsible poly(vinyl)pyrrolidone (PVP)[21] matrices, crystallizing lactose and milk systems, and vegetable tissues showing intermediate degrees of collapse, due to the presence of water-insoluble polymers that provided structural support [82,104,105]. Figure 5 [82,92,104] illustrates the main results observed for the Maillard reaction rates in lactose and apple systems, in relation to the respective phase/state diagrams, as a function of the mass fraction of water (w_1). The experimental areas investigated are shaded in gray, and the maximum rates are represented by the patterned bands in Fig. 5. The corresponding T_g curves and the solubility curves for lactose and the main soluble sugars in apple (i.e., the components that determine the T_g values for fruits and vegetables) were included for reference.

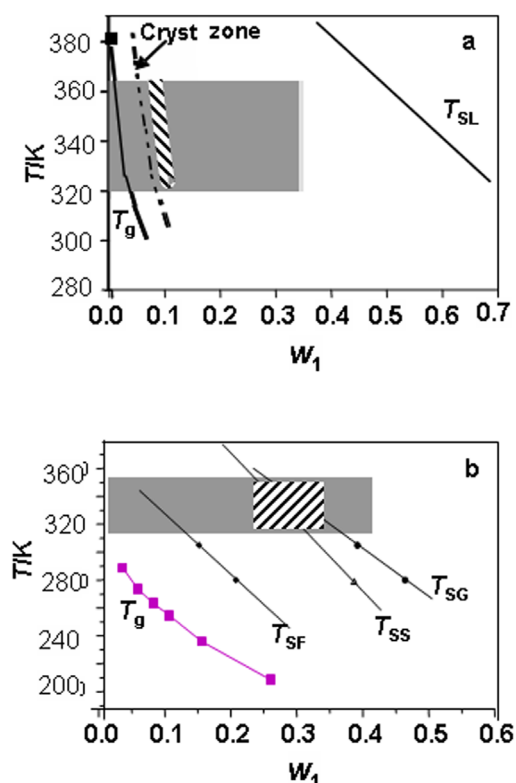[21]poly[1-(2-oxo-1-pyrrolidinyl)ethylen]

Fig. 5 State diagrams for lactose (a) and apple (b) systems, showing the experimental T_g curves and solubility data T_{SL}, T_{SG}, T_{SS}, T_{SF} for the main sugars of each system (included for reference): lactose (a) and glucose, sucrose and fructose (b), respectively, as a function of the mass fraction of water (w_1). Gray rectangles delimit the ranges of experimental conditions analyzed. The regions where the Maillard reaction exhibited its maximum rate are shown as patterned bands [82].

The rate of browning in the analyzed fruit and food models was very low in the glassy state, but at temperatures above T_g, in addition to decreasing viscosity and increasing reaction rate, other changes such as crystallization and collapse affected the Maillard reaction rate. The minimum water content at which browning was detectable was not directly related to the water hydration limit (or "monolayer" value), calculated through the Guggenheim, Anderson, and de Boer (GAB) equation [106], nor to the T_g values of the systems. Table 2 shows that in various foods and model systems stored at 343 K, the maximum Maillard reaction rates were reached either close to or well above T_g, according to the structure of a given system [104].

The observation of a maximum rate as a function of water mass fraction indicated that the reaction rate decreased at a point at which the matrix was unable to absorb additional water, either because of crystallization (as in the case of lactose-containing systems, Fig. 5a), by saturation of the most active sites in the water-absorbing matrix (as in the case of vegetable tissues, Fig. 5b). The inhibitory water concentration appeared to be associated with the saturation of the second sorption stage (as analyzed by an inverse plot of the GAB model, as proposed by Timmermann and Chirife [106]). Upon the first appearance of frozen water and highly mobile water (determined by spin–spin transverse relaxation time, T_2, analyzed by ^{1}H NMR, using the Hahn pulse sequence [105]), the Maillard reaction rate decreased [105]. The water content at which the rate of the Maillard reaction is a maximum results from a compromise between plasticization by water and water's inhibitory effect.

Table 2 Difference between storage temperature and glass-transition temperature ($T-T_g$), water activity (a_w) and mass fraction of water (w_1) values corresponding to the maximum Maillard reaction rates in various foods and model systems stored at 343 K (from ref. [104]), and the corresponding physical structure.

Matrix	a_w	w_1	$(T-T_g)$/K	Physical structure
PVP	0.25–0.38	0.11	0–5	Fully collapsed, liquid-like, not crystallized
Lactose	0.33–0.52	0.04–0.07	30–50	Crystallized
Lactose/starch	0.33–0.52	0.05–0.07	56–64	Partly crystallized
Milk	0.43–0.75	0.07–0.08	40–60	Partly crystallized
Apple	0.45–0.57	0.13–0.17	100–130	Caked, soft
Chicken meat	0.43–0.52	0.07–0.09	80–90	Caked
Cabbage	0.52–0.75	0.12–0.23	99–130	Sticky
Potato	0.70–0.80	0.13	100–120	Caked, tough

3.4 Degradation of encapsulated hydrophobic components

Stability and retention of labile biomolecules during drying and later storage are often dependent on their encapsulation in an amorphous matrix formed during dehydration processes [23,107]. Amorphous sugars are effective encapsulating agents. However, sugar crystallization, as a consequence of storage above T_g, promotes both the release of encapsulated lipids [108,109] and the loss of any stabilizing effect on biomolecules such as enzymes [80]. The changes in the physical structure of a matrix may also lead to increased permeability and diffusivity of gases (H_2O, O_2) that can affect reaction rates and decrease the stability of encapsulated active materials [110–112].

In noncrystalline polymeric matrices, the release of encapsulated material has been qualitatively related to structural collapse or shrinkage, as a result of storage above T_g of the matrix [113–116]. However, Prado et al. [117] found that β-carotene[22] losses were mainly observed in the glassy state (below T_g), where a high-porosity amorphous matrix allowed oxygen diffusion and then a fast β-carotene degradation. In contrast, lower degradation rate constants were observed under conditions in which the matrix was fully plasticised, and consequent structural collapse caused the disappearance or dramatic reduction of micropores in the matrix. The effect of molar mass of maltodextrins and the efficiency of different drying methods on the retention of β-carotene have also been investigated. Maltodextrins improved the shelf-life of β-carotene, in comparison to carrot juice spray-dried without maltodextrins [118]. In the case of oxidizable compounds, the porosity of freeze-dried amorphous systems may negatively affect the stability of encapsulated compounds [117]. Elizalde et al. [119] showed that the rate of loss of encapsulated β-carotene in a trehalose matrix was mainly affected by the excess of moisture above that necessary for trehalose dihydrate crystallization. Once crystallization was completed, the kinetics of β-carotene loss were strongly accelerated.

3.5 Structural effects related to chemical stability

Acevedo et al. [120] showed that the different structures generated during drying of apple discs, as determined by the type of drying method (air convection or different freezing rates prior to freeze-drying), affected sorption properties of the dried material, and consequently, the rate of browning devel-

---

[22]5,6:5',6'-diseco-β,β-carotene-5,6,5',6'-tetrone

opment, which in turn was also different from that for dried apple powder samples. As mentioned earlier, water is one of the products of the Maillard reaction. The increase in water content resulting from the Maillard reaction is reflected in a depression of T_g [73,121]. Water is also released as a consequence of crystallization of certain amorphous sugars, and both accelerated enzyme inactivation and browning development can result [122,123]. The magnitude of that effect was dependent on the degree of matrix collapse or porosity, which affected water retention in those systems [61,121].

An inverse correlation was observed between degradation rate constants for β-carotene and degree of matrix collapse [117]. Thus, matrix collapse under controlled conditions during product processing can lead to improved stability of encapsulated biomolecules. These observations revealed that factors such as matrix microstructure and porosity may be important modifiers of reaction kinetics, and these aspects are related to the location of system conditions in the state diagram.

4. PRACTICAL ASPECTS

The phase/state transition behavior of food solids and many pharmaceutical formulations has similarities to that of synthetic polymers [2]. Water is probably the most significant diluent and plasticizer in such systems [2], and significantly affects the physical state and properties of other system components [20].

As discussed in previous sections, the establishment of the state diagram requires knowledge of three main temperature curves as functions of the mass fraction of solids:

* the freezing point depression curve
* the solubility curve
* the glass-transition curve

In the recently published Part I of this report, Corti et al. [29] analyzed theoretical and empirical models that have been applied to predict equilibrium and non-equilibrium transition temperatures in aqueous systems. The required information to create supplemented phase/state diagrams for simple binary or ternary aqueous systems can be obtained from literature data for single components, complemented by the application of theoretical or empirical relationships analyzed by Corti et al. [29]. Food systems represent a higher degree of complexity, but their physical state is usually governed by phase transitions of the main components, i.e., carbohydrates, lipids, proteins, and water [21]. A first approximation of a state diagram can be generated on the basis of system composition (main soluble components, insoluble biopolymers, and water content), and of available literature on the critical points of their typical thermal or mechanical transitions. Then, the occurrence or not of some phenomena and their kinetics in this latter case can be predicted by the relative position of the curves in the supplemented state diagram and the experimental conditions at which the systems will be exposed.

4.1 Food systems

Sugars are the main soluble components that determine the T_g values in vegetable and dairy systems, and the latter can be restricted to a description of the state of lactose. The glass-transition and solubility curves for the main component sugars may thus be employed as references in such systems; the location of the $(T_g'; w_g')$ point and the dependence of T_g on water content, described by the coefficient of the Gordon–Taylor equation, k_{GT} (Section 5.2), are important tools for defining the phase/state diagrams [6]. Table 3 shows several literature citations in which T_g', w_g' values have been reported in the literature for various food systems. In most of them, also the k_{GT} values are provided. These data are very valuable in order to have a first approximation of the potential state of a given system at given conditions.

Table 3 Literature sources in which T_g', w_g' for the maximally cryoconcentrated matrix, T_m' and the Gordon–Taylor coefficient, k_{GT} were reported.

	Food	Reference
Vegetables and fruits	Onion	252
	Grape	
	Garlic	253
	Pineapple	190
	Tomato	124, 254
	Plum skin and pulp	125
	Date flesh	255
	Apple	256, 257
	Kiwifruit	258
	Chinese gooseberry	259
	Persimmon	260
	Camu-camu	261
	Raspberry	262, 263
	Blueberry	263
	Strawberry	12, 253
	Grapefruit	264
Grains and seeds	Cereal proteins	9, 138
	Waxy corn starch	15, 209
	Rice	265
Dairy products	Skim milk	75, 88
	Whole milk	75, 210
Meats and fish	Chicken meat	265
	Abalone	146
	Chicken	147, 201
	Mutton	147
	Tuna	267
	King fish	145
	Carp surimi	268, 269
	Cod	270
	Mackerel	269
	Beef muscle	201, 271
	Pork muscle	201
	Grouper fish	286

As recently discussed by Reid and Fennema [201], fixing the exact location of the intersection of the equilibrium ice-melting with the glass-transition curves, however, has been a subject of considerable controversy. Thus, readers should be alerted to the fact that sometimes the literature is inconsistent in the nomenclature of T_g', T_m' and sometimes other reference temperatures are defined. Figures 1 and 2 illustrate the most simple, consistent, and objective presentation of several views, agreed by the

authors of the present report, and can help to interpret or analyze the original sources of data and decide which variable is being referred to, on the basis of the discussions in Section 2.

4.1.1 Fruit and vegetable tissues

Ice-melting temperatures, specific heat capacities, and unfrozen water contents are reported in most of the papers cited in Table 3. In all cases, the Gordon–Taylor equation adequately describes the dependence of T_g on the mass fraction of water at $a_w \leq 0.90$. At higher a_w values, the effect of freeze-concentration led to an increased T_g. Annealing of samples allowed devitrification of water and thus a minimal amount of non-frozen water in the amorphous matrices, a gradual disappearance of the ice-formation exotherm, and a consequent increase in the area of the ice-melting endotherm. The unfrozen water content at each condition was determined from the dependence of melting enthalpy on sample mass fraction of water. Some authors [124,125] reported that at $a_w \leq 0.75$, two glass transitions were observable for certain fruit tissues. The first T_g was attributed to the amorphous matrix formed by sugars and water. The second one, less pronounced and less affected by water content, was attributed to macromolecules of the fruit pulp. The state diagrams and water-sorption properties of various fruits and vegetables were useful in determining critical points for physical stability, and also for optimizing the retention of nutrients (anthocyanins, phenolics, and antioxidants) [references in Table 3].

Spray-dried asaí (tropical fruit) showed k_{GT} values of 4.60, 3.75, 3.56, and 6.87, depending on the type of excipient: maltodextrin of dextrose equivalent (DE) 10, maltodextrin DE 20, gum arabic, or tapioca starch, respectively [71], thus suggesting the possibility of improving material stability by incorporating appropriate ingredients.

4.1.2 Dairy products

Vuataz [75] has presented a very complete overview of the applicability of phase/state diagrams for optimizing the drying and storage of milk products, including practical aspects. He used the following tools:

- The freezing-point-depression curve described in the literature [75,126], up to a certain w_2.
- The solubility curve, based on the solubility of lactose in water [75], and according to a hypothesis on the partitioning of water, in order to dissolve milk ingredients (mainly the proteins and salts).
- T_g values of skim, half-skim and full-cream milk powders vs. powder a_w (measured at 25 °C) determined by differential scanning calorimetry (DSC) [75]. The relationship was linear in the range of a_w between 0.1 and 0.3 and allowed description of the behavior of the whole range of fat contents, with the same lactose to protein ratio. Moreover, this linear relationship was rather similar to the line established for pure amorphous lactose [127] and for spray-dried whey powders with various degrees of lactose precrystallized in the α-hydrate form. Vuataz [75] identified the region of the phase diagram manifesting a high risk of crystallization. From an examination of several works on the glass-transition values for dehydrated skim milk and lactose-based model systems, it can be concluded that the T_g of skim milk powders, detectable by DSC, is governed by the T_g for lactose [88,123,128,129]. The addition of maltodextrin raised the T_g of dairy-based food powders [121,130].

4.1.3 Cereal products

Starch, proteins, and water are the main components defining the operational phase/state diagrams for cereal-based foods [7,9,11]. The structure of many cereal-based products (bread, crackers, corn flakes) can be regarded as a tri-dimensional continuous network of proteins containing a discontinuous (or interpenetrating) phase composed of starch granules exhibiting a variable degree of organization, depending on the processing conditions for the particular type of product [7,9,11]. It is interesting to note that the main thermomechanical changes in the final product frequently occur in the starch phase. Thus, phase/state diagrams for cereal products are often constructed in terms of starch [2]. However, product structural stability is typically controlled by the continuous protein phase. The thermal transi-

tions of the protein phase are meaningful in establishing the process conditions that generate the expected properties [7], while the thermal transitions of the starch phase often define product storage stability [9].

Starch is a partially crystalline polymeric material (as observed by X-ray diffraction) that is organized in granules. When heated in the presence of sufficient water, the granules swell, and the crystalline organization in starch is destroyed at a characteristic temperature. This molecular disordering process is called gelatinization; it can be observed as an endothermic event, by DSC, and can also be reflected in the X-ray diffraction pattern of a starch-containing material [1,131]. Gelatinization can be related to the melting phenomenon for semi-crystalline polymers [1]. Thus, phase/state diagrams for starch-containing systems can be constructed from the ice-melting curve, the gelatinization curve, and the T_g curve for starch [2].

The T_g values for anhydrous high-molecular-weight food polymers such as polysaccharides [16,132] and proteins [133–135] are usually high [6], and such materials tend to decompose at temperatures below their T_g [16]. Although the T_g values for starch, gluten protein [7,133], glutenin [134], and amylopectin-protein mixtures [128] are important in the characterization of various extruded and other cereal-based foods [2] the experimental values for many anhydrous food polymers cannot be experimentally determined. Based on the T_g values for maltodextrins, Roos and Karel [17] predicted a T_g value for anhydrous starch of 516 K, which was close to the previously reported value, 516 K [131].

Slade and Levine [1] analyzed the T_g and effective "end of non-equilibrium melting temperatures" (corresponding to the solubility curves in Figs. 1 and 2) for amylopectin microcrystallites in normal wheat and waxy corn starches by DSC. Results of that study explained the kinetically controlled relationship (based on the dynamics of plasticization by water) between the operative temperature, at which a non-equilibrium process of annealing can occur in native granular starches subjected to various heat/moisture/time treatments, and the effective T_g and T_s relevant to gelatinization [1]. They also demonstrated that the effective T_g associated with gelatinization of native granular starch depends on the mass fraction of water, temperature, and time, because the glass transition represents a rate-limiting stage of a relaxation process [1]. This rate-limiting stage depends on the instantaneous magnitudes of free volume and/or local effective viscosity. These magnitudes depend in turn on the relative values of experimental water content compared to the water content of the operative glass, experimental temperature compared with the instantaneous T_g, and experimental time frame compared with the instantaneous relaxation rate [1]. Such a relaxation process, described by WLF free volume theory for glass-forming systems, underlies various functional aspects of starch, such as gelatinization, crystallite melting, annealing, and recrystallization [1,2].

Bread is an unstable, elastic, solid foam, the solid part of which contains a continuous phase, composed of an elastic network of cross-linked gluten molecules and of leached starch polymer molecules, primarily amylose (complexed or not with polar lipid molecules), and a discontinuous phase of entrapped, partially gelatinized, swollen, deformed starch granules [136]. Starch gelatinization induces major structural changes during the baking of wheat bread. The swollen granules and partially solubilized starch act as essential structural elements of bread [137]. The other important functional component of wheat flour is gluten protein, which is responsible for the formation of the viscoelastic gluten network in dough. On heating, gluten transforms from a thermoplastic, entanglement gel to a thermoset, intermolecularly crosslinked/polymerized gel network [7]. Thus, the transformation from dough to bread involves changes in both the starch and protein fractions [7,137].

The glass transitions of zein protein from corn, gliadin, and glutenin (the two components of wheat gluten) have been studied as functions of the mass fraction of water, using mechanical spectrometry and DSC [138]. All three of these cereal proteins are plasticizable by water, suggesting that their hydrophilic domains play an important role in determining their rheological properties at low water contents. The dependence of T_g on water content for each protein could be predicted by the Gordon–Taylor equation. Temperature sweeps using small-amplitude oscillatory measurements suggested that all three proteins undergo crosslinking reactions in the temperature range 70–160 °C; above

160 °C, all proteins showed characteristic softening [138]. The development of state diagrams for such cereal proteins can thus be used to predict their behavior during processes such as baking and extrusion [2,9].

The thermal transitions occurring during the baking and storage of bread have a profound impact on bread's structural characteristics [139]. According to relationships established for synthetic polymers, which are also valid for biopolymers [2], the viscosity of such food systems depends on the difference between the temperature of the system and its T_g [9]. Staling can be defined as a group of changes that take place during bread storage, due to certain physicochemical transformations [140], which result in an increased crumb firmness, changes in flavor and aroma, and loss of crispiness. Bread firming is mainly caused by recrystallization of the gelatinized starch fraction [2], involving amylopectin chains [141], and also by starch–gluten interactions [142]. As an example of the applicability of phase/state diagrams in the prediction of food quality aspects, Fig. 6 shows a state diagram illustrating the evolution of two starch-containing dough systems during bread making (from dough A to final product) [143]. T_{s1} and T_{s2} represent the gelatinization temperatures for two formulations containing corn starch and other biopolymers. In both cases, the final product lies in the supercooled region (between the T_s and T_g curves) at room temperature, and starch recrystallization (staling) would be possible for both formulations. The maximum recrystallization rate depends on the relative positions of the glass-transition and gelatinization curves (as discussed in Section 2). Thus, a change in formulation affecting one of the curves (gelatinization, in this case) produces that staling for formulation 1 is delayed. Since in the absence of gluten starch retrogradation is accelerated, these concepts can be helpful in the development of formulations for gluten-free breads.
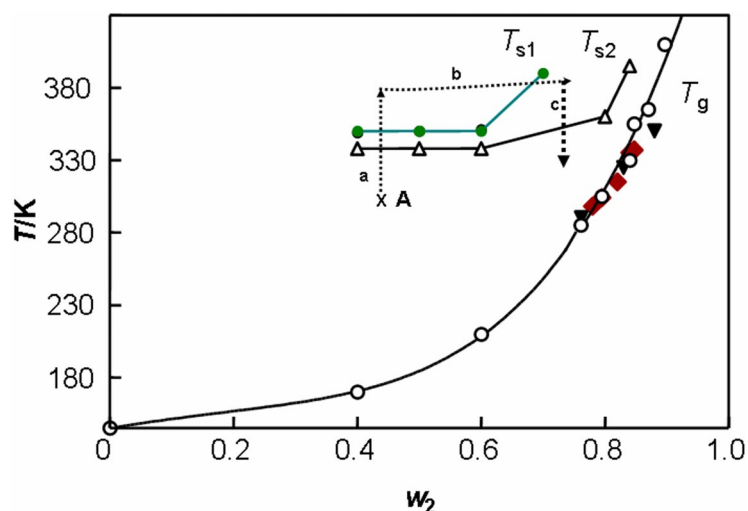

Fig. 6 Schematic state diagram, based on a starch-containing aqueous systems, for two bread dough formulations having starch gelatinization temperatures of T_{s1} and T_{s2}. The T_g values for both formulations are similar and are shown as a function of the mass fraction of solids (w_2) [143]. Lines a, b, and c show the hypothetical evolution of the systems from the dough to final products.

Levine and Slade [11] used state diagrams to analyze different aspects governing cookie texture. Formulation and baking time and temperature can define the location of a final product on a state diagram, and consequently, a product's texture attributes and storage stability at a fixed temperature [5,11]. These workers demonstrated the major opportunity offered by their "food polymer science" approach to expand not only quantitative knowledge, but also, of broader practical value in the context of indus-

trial applications, qualitative understanding of (a) the functionality of flours and flour components, and (b) the importance of glassy and rubbery states, in commercial cookie products and processes [7,9,11].

4.1.4 Sugar confectionery

The candy industry was developed largely on an empirical basis. Nevertheless, the different steps followed during candy making can demonstrate numerous principles of physical chemistry, polymer science, and engineering [144]. Additional knowledge of the principles of binary-component phase/state diagrams may allow one to identify the location of the different steps in such diagrams. Figure 7 shows the schematic steps that a system may follow to produce different types of sugar-based confectionery products.
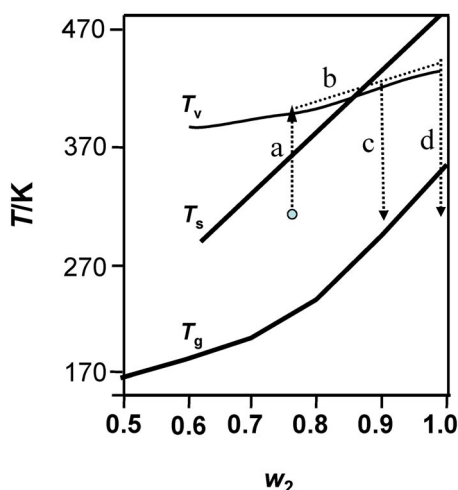

Fig. 7 State diagram illustrating the several stages in the production of sugar confectionery: a glassy hard-boiled candy (lines a → b → c), or a supercooled soft candy (lines a → b → d). Lines T_v, T_S, and T_g represent the boiling point, solubility, and glass-transition temperatures, respectively, as a function of solids mass fraction (w_2).

Sugar confectionery products are produced by dissolving sugar in a limited amount of water, via warming up to an appropriate temperature (T_s) at which all the sugar can be solubilized (line a in Fig. 7). Upon further heating (line b), water is evaporated along the boiling-point curve. Depending on the degree of achieved concentration (lines c or d in Fig. 7), a soft product (like toffee or fudge, line c) or a glass (hard-boiled candy, line d) is obtained upon cooling back to ambient temperature. In candy making, many different kinds of products can be produced by appropriate selection of temperatures, final concentrations, agitation, and cooling rates. In the supercooled region between T_s and T_g, fast cooling and agitation can promote a fast nucleation rate and the formation of small crystals, for a soft texture. The presence of milk solids and gums can also affect the extent of sugar crystallization. The formation of a small amount of large crystals (as in the case of rock candies) is favored by the avoidance of agitation, of the presence of impurities, and by very slow cooling. As already noted, the confectionery industry has developed many products largely on an empirical basis. However, with the help of information provided by phase/state diagrams [38], fewer trial-and-error experiments can lead to desired products. Confectionery products represent an example of simple systems (basically composed of sucrose, water, and possibly milk solids, for example), with transitions very easily detectable by DSC, from which a great variety of products can be obtained, if the kinetics of sugar crystallization are appropriately controlled. The main variables that must be controlled are: heating temperature, time of heat-

ing (concentration), cooling and agitation rates, and of course, packaging and storage conditions. A wide variety of confectionery products are obtained by careful control of these variables.

4.1.5 Animal tissues

In DSC thermograms for fish products, Sablani et al. [145] noticed an endothermic peak, attributed to the melting of oil, and a shift in baseline, which they attributed to a glass–rubber transition. This baseline shift was difficult to identify by DSC, for samples equilibrated at different a_w values (corresponding to water mass fraction ranging from 0.09 to 0.28), and increasing water had little influence on the location of the T_g range, i.e., the plasticizing effect of water on fish protein was very small.

Sablani et al. also developed a state diagram for abalone [146]. Freezing points were determined by the cooling method, and the T_g values were measured by dynamic oscillation in shear [146]. The limited glass-transition process of the abalone network needs derivation of a mechanical T_g, since the transition could not be detected using modulated DSC (MDSC). Sunooj et al. [147] illustrated how several parameters, such as annealing temperature and time employed, sample water content, rate of heating during DSC scan, etc., can affect the calorimetric determination of T_g for complex food systems such as chicken and mutton. As annealing temperature decreased from −11 to −23 °C, T_g values for chicken and mutton tissues shifted toward lower temperatures. Similarly, annealing times up to 1 h also significantly influenced T_g values. This kind of study helps in optimizing DSC protocols for calorimetric determination of T_g for animal tissues.

4.2 Pharmaceutical systems

Therapeutic proteins (e.g., erythropoietins, insulin, monoclonal antibodies, blood factors, and interferons) constitute the most rapidly growing class of pharmaceuticals for use in several clinical situations, including cancer, chronic inflammatory diseases, kidney transplantation, cardiovascular medicine, and infectious diseases [148].

Injectable aqueous solutions are often the most convenient and preferable dosage form for therapeutic proteins, whereas many purified proteins are not sufficiently stable in solution to meet shelf-life requirements, even when they are stored at low temperatures [149]. Deteriorative changes, discussed earlier in Section 3.2, can lead to a decrease in functionality and may cause an immunological response. Effective commercialization of protein pharmaceuticals requires the development of new formulations that maintain the integrity of the purified protein during the manufacturing process, distribution, and storage [149].

In the case of protein pharmaceuticals, a supplemented state diagram can help in

- selecting appropriate excipients;
- selecting operating conditions for freezing and freeze-drying; and
- selecting storage conditions.

Typical formulations for modern pharmaceutical freeze-dried proteins contain excipients (e.g., sugars, polymers, amino acids) that can protect proteins from damaging physical and chemical changes [149]. Examples of excipients appropriate for use during freezing and/or freeze-drying are listed in Table 4.

Table 4 Examples of excipient components in pharmaceutical formulations for therapeutic poteins.

	Trivial accepted name	IUPAC systematic name
Sugars	Trehalose	(2*R*,3S,4S,5*R*,6*R*)-2-(Hydroxymethyl)-6-[(2*R*,3*R*,4S,5S,6*R*)-3,4,5-trihydroxy-6-(hydroxymethyl)oxan-2-yl]oxyoxane-3,4,5-triol
	Mannose	(3S,4S,5*R*,6*R*)-6-(Hydroxymethyl)oxane-2,3,4,5-tetrol
	Sucrose	(2*R*,3*R*,4S,5S,6*R*)-2-[(2S,3S,4S,5*R*)-3,4-Dihydroxy-2,5-bis(hydroxymethyl)oxolan-2-yl]oxy-6-(hydroxymethyl)oxane-3,4,5-triol
	Glucose	(2*R*,3*R*,4*R*,5S,6*R*)-6-(Hydroxymethyl)oxane-2,3,4,5-tetrol
Polyols	Sorbitol	(2S,3*R*,4*R*,5*R*)-Hexane-1,2,3,4,5,6-hexol
	Mannitol	(2*R*,3*R*,4*R*,5*R*)-Hexane-1,2,3,4,5,6-hexol
	Glycerol	Propane-1,2,3-triol
Amino acids	Histidine	(*S*)-2-Amino-3-(1*H*-imidazol-4-yl)-propanoic acid
	Aspartic acid	2-Aminobutanedioic acid
	Arginine	(*S*)-2-Amino-5-(diaminomethylidene amino)pentanoic acid
	L-Glutamine	(2S)-2-Amino-4-aminocarbonyl-butanoic acid
	Glutamic acid	(S)-2-Aminopentanedioic acid
	Alanine	(*S*)-2-Aminopropanoic acid
	L-Glycine	(*S*)-2-Aminoethanoic acid
	L-Lysine	(2S)-2,6-Diaminohexanoic acid
Proteins	Gelatin	–
	Albumin	–
Polymers	Inulin (polydisperse blend of fructose polymers)	(2*R*,3S,4S,5*R*)-2-[[(2*R*,3S,4S,5*R*)-3,4-Dihydroxy-2,5-bis(hydroxymethyl)oxolan-2-yl]oxymethyl]-5-(hydroxymethyl)oxolane-2,3,4-triol
	Pullulan (1,4-1,6-α-D-Glucan, 1,6-α-linked maltotriose)	–
	Hydroxypropyl-β-cyclodextrin	2-Hydroxypropyl-β-cycloheptapentylose
	Polysorbate	2-[2-[3,4-bis(2-Hydroxyethoxy)oxolan-2-yl]-2-(2-hydroxyethoxy)ethoxy]ethyl dodecanoate

Disaccharides (e.g., sucrose, trehalose) are among the most popular sugar excipients, because they are believed to stabilize proteins both thermodynamically [26,51] and kinetically [45] in aqueous solutions and freeze-dried solids. Aqueous sugar glasses are widely used to stabilize proteins during drying and subsequent storage [28,31]. The required properties of sugars that function successfully as protectants are: a high T_g, low hygroscopicity, a low crystallization rate, and an absence of reducing groups.

Table 5 shows some typical formulations used to protect selected proteins. Many of these formulations include amino acids and/or carboxylic acids in combination with saccharides.

Table 5 Examples of excipients appropriate for protecting selected proteins during freezing and/or freeze-drying.

Protein	Excipient	Reference
Catalase (bovine liver)	Maltose + phosphate buffer	270
β-Galactosidase	Mannitol, sodium phosphate	160
β-Galactosidase	Inositol + phosphate buffer	163
β-Galactosidase	Several maltodextrins, trehalose, PVP, and starch	96
Alcohol and glutamate dehydrogenases (ADH, GDH)	Trehalose + KCl + KH_2PO_4 + mannosylglycerate	271
Human serum albumin	Mannitol + NaCl	272
Bovine serum albumin	Trehalose	273
Tissue plasminogen activator	L-Arginine + multivalent inorganic acids	148
Human growth hormone	Mannitol, trehalose, and cellobiose	23
Recombinant human growth hormone	Mannitol and glycine	23
Chymotrypsinogen	Sucrose	273
Bovine and human insulins	Dextrin, dextrose, and hydroxypropyl β-cyclodextrin; mannitol + HPBCD	52
Recombinant factor IX	Polysorbate 80, sucrose, and histidine	275
Recombinant human interleukins	Trehalose, sucrose and hydroxyethyl starch; sucrose, glycine and mannitol	276
PFK (phosphofructokinase)	Sugars (sucrose, lactose, maltose, trehalose) + salts (NaCl, KCl)	49, 50
Recombinant human interleukin-1 receptor antagonist	Sucrose, sorbitol, trehalose, and alanine; mannitol and glycine, sodium citrate	276
Recombinant human albumin	Organic acids	278
Lactate dehydrogenase, phosphofructokinase	Polyethylene glycol; sugars (lactose, mannitol, and trehalose)	279
Lactate dehydrogenase	Hydroxypropyl β-cyclodextrin (HP-β-CD), sucrose ester, buffer	148, 150
Lactate dehydrogenase	Succinic, tartaric, malic acids + L-histidine, arginine, and glutamic acid	147
Alkaline phosphatase	Lactose, mannitol, and trehalose	280
Alkaline phosphatase	Inulin	152
Recombinant human somatropin, lysozyme	Sucrose, sorbitol, and glycerol; sorbitol	281 282
Lactoferrin	L-Arginine, trehalose, tween, and phosphates	154
Subtilisin	Sucrose, trehalose, dextran, and maltodextrin	283

Amorphous glassy solids formed by freeze-drying of disaccharides and/or amino acids are said to protect proteins from structural changes thermodynamically by substituting for surrounding water molecules [26,51]. They also inhibit chemical degradation of freeze-dried proteins kinetically by reducing molecular mobility [45]. In addition, some amino acids (e.g., L-arginine[23]) prevent protein aggregation in aqueous solutions prior to drying and after reconstitution [149].

---

[23](S)-2-amino-5-(diaminomethylidene amino)pentanoic acid

The development of freeze-dried protein formulations containing amino acids is often more challenging than is the development of formulations containing saccharides, because of the former's more unusual physical and chemical properties (e.g., crystallinity, very low T_g values), as well as their tendency to form complexes with other ingredients [150]. Choosing appropriate counterions that form glassy-state solids should be one of the key factors in designing amino acid-based amorphous freeze-dried formulations. For example, the T_g values for freeze-dried L-histidine[24] and L-arginine salts depend largely on the particular counterions [149–151]. Co-lyophilization of L-arginine and multivalent inorganic acids (e.g., H_3PO_4) results in amorphous glassy solids that protect proteins during processing and storage (e.g., tissue plasminogen activator formulation [151]). Some organic acid and inorganic cation combinations (e.g., sodium citrate) also form high-T_g amorphous solids [148]. Various functional groups (e.g., amino, carboxyl, hydroxyl) in the constituting molecules contribute significantly to the formation of glassy-state amorphous salt solids [149]. Multiple amino, carboxyl, and hydroxyl groups in the solute molecules have been found to result in elevated transition temperatures for the frozen solutions (T_g') and freeze-dried solids (T_g) [149,151]. Differently protonated carboxyl and carboxylate groups also form an intermolecular hydrogen-bonding network. Basic amino acid- and organic acid-combination freeze-dried solids should provide embedded proteins with unique local environments that are significantly different from those of non-ionic excipients (e.g., saccharides). Enzymes such as L-lactate dehydrogenase[25] (LDH), alkaline phosphatase[26] (AP), and phosphofructokinase[27] (PFK) are often used as models for studying the effects of freeze-thawing and -drying processes, because of their tendency to lose their activities [149]. The capability of excipient combinations to retain enzyme activity during freeze-drying is evidenced for the stabilization of tertiary and quarternary structures against freeze-concentration and dehydration stresses.

T_g values for anhydrous pentoses, hexoses, disaccharides, and alditols, their T_g' values, concentrations of their maximum cryoconcentrated matrices, and changes in specific heat at T_g (ΔC_p) have been compiled by Corti et al. [29]. Roos [21,152] also included melting-temperature values of the dry compounds. Some such information, for amino acids and carboxylic acids, is provided in the references shown in Table 6. As discussed in relation to Table 3, the analysis of data sources on the basis of concepts introduced in Section 2, and Figs. 1 and 2, is encouraged.

When freeze-drying is selected as the method of choice for drying, a relatively high T_g value of the freeze-concentrated fraction (T_g') is preferred. Hinrichs et al. [153] evaluated inulins[28] of various degrees of polymerization (DP), in comparison to trehalose. They found that the T_g and T_g' values for inulins with number/weight-average DP (DPn/DPw) ratios higher than 5.5/6.0 were higher than those for trehalose glasses. Freeze-drying of an AP solution without protectant induced an almost complete loss of enzyme activity. In contrast, when inulins with DPn/DPw higher than 5.5/6.0 or trehalose were used as stabilizers, enzyme activity was fully maintained, even after subsequent storage for 4 weeks at 20 °C at relative humidities between 0 and 60 % (being relative humidity defined as 100 a_w). The stabilizing capacities of glucose and of inulin with lower DP were substantially less pronounced. It was concluded that inulins with DPn/DPw higher than 5.5/6.0 meet the physico-chemical requirements of successful protectants for proteins [153].

---

[24](*S*)-2-amino-3-(1*H*-imidazol-4-yl)-propanoic acid
[25]E.C. number 1.1.1.27, (*S*)-lactate:NAD$^+$ oxidoreductase
[26]E.C. number 3.1.3.1, phosphate-monoester phosphohydrolase (alkaline optimum)
[27]E.C. number 2.7.1.11, ATP:D-fructose-6-phosphate 1-phosphotransferase
[28](2 → 1)-β-D-fructofuranan; (2*R*,3*S*,4*S*,5*R*)-2-{[(2*R*,3*S*,4*S*,5*R*)-3,4-dihydroxy-2,5-bis(hydroxymethyl)oxolan-2-yl]oxymethyl}-5-(hydroxymethyl)oxolane-2,3,4-triol

Table 6 Literature sources for T_g and T_g' data for selected amino acids and organic acids or their salts, used in pharmaceutical formulations for therapeutic proteins.

Compound	Reference
Arginine[a]	150
	283
Histidine[a]	149
L-Glutamine[a]	149
L-Lysine[a]	148, 149
Glycine[a]	105
Alanine[a]	44
Glutamic acid[a]	149
Citric acid[b]	149
Tartaric acid[c]	149
Malic acid[d]	149
Histidine/citric acid	149
Sodium acetate[e]	149
Sodium citrate	149
Potassium acetate	149
Potassium citrate	149

[a]See Table 4 for IUPAC systematic names.
[b]2-Hydroxypropane-1,2,3-tricarboxylic acid.
[c]2,3-Dihydroxybutanedioic acid.
[d](S)-Hydroxybutanedioic acid.
[e]Or sodium ethanoate.

Among polyols, mannitol[29] is a popular excipient used in freeze-dried formulations to stabilize various biomolecules (e.g., proteins, enzymes, hormones, vitamins). Mannitol crystallization profiles, including those for its various polymorphs, have been studied extensively [154–158]. Chemical stability at extreme pH conditions may provide amorphous mannitol some advantages, among various other polyols and saccharides [159]. Amorphous mannitol is said to protect protein conformation during freeze-drying through hetero-solute molecular interaction with proteins (e.g., hydrogen bonding) [26,160–162]. However, obtaining pure amorphous mannitol by rapid cooling of a hot solution or by freeze-drying of an aqueous mannitol solution, while possible, is not practical, because amorphous mannitol is physically unstable and will transform into a more stable crystalline form, even under ambient conditions [159,163]. Another, more practical approach is the freeze-drying or rapid cooling of mannitol in combination with other amorphous components [107,159]. Molecular-level mixing with other components may limit the spatial rearrangement of mannitol molecules required for crystallization. In fact, various solutes that can remain amorphous in frozen solutions and during freeze-drying (e.g., NaCl, K_2HPO_4, L-glycine[30]) were reported to inhibit mannitol crystallization [23,159–168]. Altering molecular mobility in an amorphous phase by complex formation and/or molecular interaction is another approach to prevent mannitol crystallization. For example, addition of a small amount of boric acid or sodium tetraborate to a hot manitol solution retards mannitol crystallization from the resulting amorphous solid [163,169]. It has also been shown that the addition of divalent cations and

---

[29]($2R$,$3R$,$4R$,$5R$)-hexane-1,2,3,4,5,6-hexol
[30](S)-2-aminoethanoic acid

transition metals enhances the stabilizing effect of sugars and polyols on proteins [49,50], and that the addition of divalent cations retards trehalose crystallization [170].

5. METHODOLOGY

5.1 Glass-transition curve

According to Wunderlich [171], the most precise determination of the T_g for polymeric materials is obtained by cooling of a melt at a specified rate and then determining the transition temperature using heat capacity, expansion coefficient, or compressibility measurements. DSC is most often the first option for analyzing phase and state transitions. It should be noted that different cooling and heating rates always give different T_g values, for all amorphous systems [172], and the specific transition temperature within a temperature range can be identified using various criteria. Since the change in heat capacity at T_g occurs in a temperature range, usually T_g values reported are either onset or midpoint temperatures, although the onset temperatures seem to be more important, because a number of changes in food properties occur rapidly above the onset of the transition [21,22]. The temperature range over which the glass transition occurs can be narrow (about 2–5 °C, e.g., for low-molecular-weight polyols and wet sugars) or wide (larger than 15 °C, e.g., for polymers and dried materials), and the glass-transition curve could be better represented by a narrow band rather than a line. There is also a variation in T_g caused by sample thermal history, which is often neglected, but hysteresis in the glass transition can be used to gain information about the thermal history of a material [21,22]. Glasses can be annealed to obtain various types of glassy solids, which may manifest different endothermal and exothermal enthalpy relaxations around the glass transition, as well as relaxations in other thermodynamic properties [20,171,173]. Frequently, a first DSC scan is performed to eliminate the endo- or exothermal enthalpy relaxations that are often associated with the glass transition of a matrix, by heating to the end of the relaxation; this can dramatically affect the determination of the onset T_g in a rescan [173]. Care should be taken, however, to avoid causing any other physical or chemical reactions during the first scan [14–16,75]. The baseline shift often observed in DSC thermograms at T_g can occur over a wide temperature range, and can have different degrees of steepness, depending on the type of material. Typically, humidified sugars and polyols show the steepest changes in heat capacity at T_g, while dry biopolymers show very broad and flat baseline shifts.

In most of the works cited in Tables 1, 3, and 6, phase/state transitions for freeze- or air-dried materials were determined over a wide range of water contents. DSC traces for such fruit and vegetable tissues, dairy products, honey, sugar-based confectionery, and whey powders showed a clearly visible shift in baseline at T_g, and state diagrams for such food samples could be defined.

In whole-milk powders, seeds, and some cereal-based foods, T_g can be difficult to detect; depending on sample water content, the glass transition may overlap with fat melting [88]. Therefore, extracting the lipids may be an alternative for analyzing the T_g curve in lipid-containing systems, if DSC is to be employed.

In freeze-dried animal tissues (e.g., beef, chicken, fish products), it can often be difficult to find a clear glass transition by thermal analysis, since other changes can interfere or the complexity of the structure can affect identification of the glass transition [145]. In a related vein, Green et al. [174] concluded that hydrated proteins may indeed be grouped among glass-forming systems, but due to their special structural features and to the disposition of water in the protein molecules, they can show great departures from thermo or rheological simplicity.

Some vegetable systems containing starch, such as date pits [175], quinoa seeds [176], and certain cereal-based foods, also can present difficulties in detecting a glass transition from DSC measurements.

Similar difficulty has also been observed in the case of native starch, due to the nature of its structure at the molecular and microscopic levels, which could lead to a small step-change or broadening of the heat capacity change at the glass transition [177,178]. In such cases, relaxations in amorphous materials can be observed from changes in dielectric, mechanical, and thermal properties below and around the glass transition. A mechanical T_g can be determined by mechanical spectroscopy (MS) or dynamic mechanical analysis (DMA). Dielectric analysis (DEA) offers another suitable alternative to DSC for determination of glass-transition curves for doughs and frozen doughs [179,180]. These dielectric and mechanical spectroscopic methods are extremely sensitive in observing relaxations as functions of frequency and temperature. Such relaxations can involve both sub-T_g relaxations, referred as β and γ transitions, and the glass transition itself, which is the main α-denoted relaxation. DEA and DMA have been employed for obtaining complementary information to DSC when analyzing glass transition and crystallization of polyols [54], subzero transitions [179,180] and sub-T_g relaxations in different carbohydrate models [54,179,180].

The basic principle of such mechanical or dielectric measurements is the application of an oscillating perturbation (a mechanical stress or an altenating electric field), at a given frequency, to a sample in a suitable disposition, and the detection of its response. The main advantage of applying such oscillating perturbations is that, due to the vectorial representation of a wave, the response may be deconvoluted into two components: one of them representing the portion of the applied energy which is stored by the material (elastic or capacitive component) and used in recovery, the other representing the applied energy that is converted to heat and lost (viscous or conductive component).

^{1}H NMR relaxation times can be also employed to analyze molecular mobility in the proximities of the glass transition. Time-resolved ^{1}H NMR is based on an analysis of the relaxation times of proton magnetic spins, after a radio-frequency pulse, when samples are located in a magnetic field. ^{1}H NMR allows one to assess differences in molecular mobility of polymers, by measuring changes in spin–spin (T_2) or spin–latice (T_1) relaxation constants, as a function of temperature or water content [181–184]. Radio-frequency pulses are designed based on the angle at which they rotate the magnetization vector representing a sample. Spin–spin relaxation times, obtained from free induction decay (FID) following a single 90º pulse, are affected by field inhomogeneities. Only the relaxation times for fast-relaxing protons (which are in the microsecond range) can be correctly measured without a 180º-refocus pulse [185]. FID analysis can thus be used to evaluate proton mobility associated with a solid matrix. Decay envelopes obtained after a radio-frequency 90º pulse can be fitted to mono-exponential behavior, and corresponding time coefficients can be obtained. T_2 values obtained by FID analysis (T_{2FID}), for corn flake samples at different water contents, showed a change in slope for T_{2FID} vs. temperature. This event occurred at a temperature close to the T_g determined by DSC [186]. DMA, DEA, and time-resolved ^{1}H NMR have thus provided alternative ways of determining T_g in various cereal-based products or systems based on starch or protein, where T_g is difficult to detect by DSC measurements. It should be noted that the various analytical methods give slightly different T_g values [20–22]. The T_g value of a single sample also depends on the sample thermal history and even the same analytical method may give varying T_g values. Thus, the specific conditions for each method should be provided. While scan rate is one of the main factors in determining a T_g value by thermal analysis, reports of T_g determined by methods involving oscillatory perturbations (e.g., DMA, DEA) should be accompanied by a clear statement of the measurement frequency and other parameters being used. For the ^{1}H NMR relaxation times, the pulses sequence and the interpulse time should be given. In addition, the application of such methods requires considerable theoretical knowledge about a given material's viscoelastic, dielectric/conductive properties and magnetic spin proton properties.

Schematic representations of changes in thermal, mechanical, electrical, and magnetic spin-relaxation times in the proximity of T_g are shown in Fig. 8.
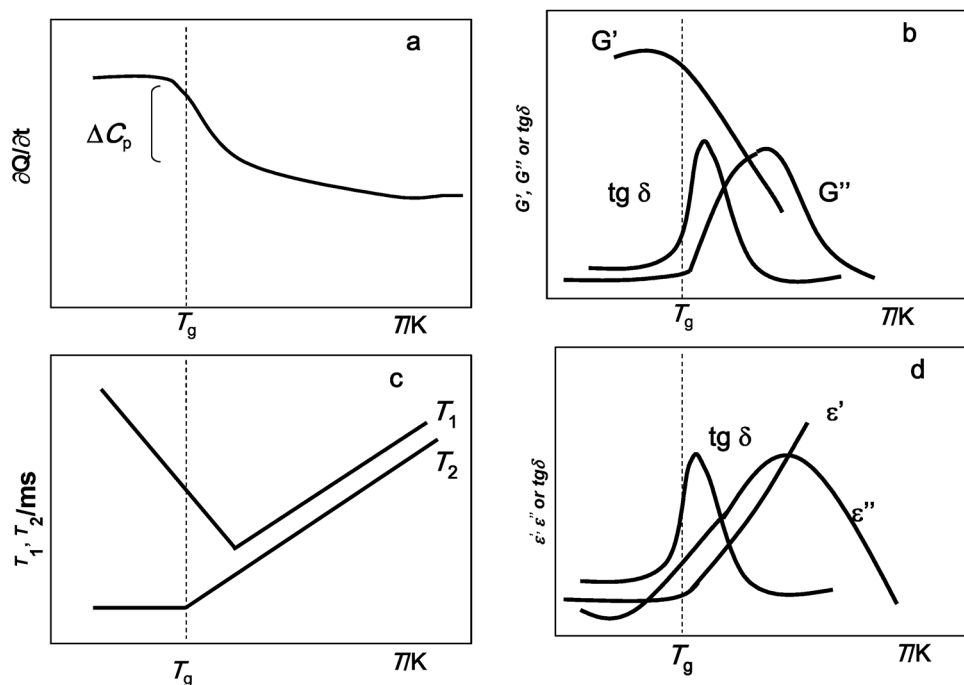

Fig. 8 Schematic representations of changes in different properties in the proximities of T_g. (a) Heat flow ($\partial Q/\partial t$) as detected by differential scanning calorimetry (DSC). (b) G', mechanical storage (elastic) modulus; G'', mechanical loss (viscous) modulus; tg δ, dissipative factor = $G''G'$, as measured by mechanical dynamic analysis (DMA). (c) Proton magnetic spin-relaxation times (^{1}H-RMN): T_1, spin-lattice (longitudinal) relaxation time; T_2, spin-spin (transversal) relaxation time. (d) ε', permittivity (proportional to capacitance); ε'', loss factor (conductive component) tg δ, dissipative factor = $\varepsilon''/\varepsilon'$, measured by dielectric analysis (DEA).

Besides T_g measurements per se, the reliability of a glass-transition curve in a state diagram depends on the accuracy of the determination of the water contents of samples. Recently, Isengaard et al. [187] published a comprehensive review of water-content measurements in foods and related systems.

5.2 T_g dependence on water content: The Gordon–Taylor equation

As discussed in Section 1 [29], several theoretical equations have been applied to describe the effect of water on T_g values, based on either volumetric, thermal, dielectric, or hydration properties. However, the Gordon–Taylor equation (2) seems to be of most general applicability to amorphous systems such as pharmaceutical and food products and components.

$$T_g = \frac{w_2 T_{g2} + k_{GT} w_1 T_{g1}}{w_2 + k_{GT} w_1} \tag{2}$$

This model requires knowledge or adjustment of the following three constants:

- The glass-transition temperature of pure water, T_{g1}. Although some uncertainty exists about this value, it has traditionally been taken as 136 K [188,189]. Corti et al. [29] have recently discussed the T_g and ΔC_p values for pure water, and possible reasons for discrepancies in the values reported by several authors.
- The glass-transition temperature of a fully dried solute material, T_{g2}. Since it is not easy to completely dehydrate an amorphous food powder, care should be taken to avoid chemical changes, partial recrystallization by heating to too high a temperature, and structural changes that can slow the diffusion of water through an amorphous matrix.
- The k_{GT} coefficient, which expresses the nonlinearity of the plasticizing effect of water.

k_{GT} is an adjustable parameter, whose magnitude provides information about specific interactions between the two components (solute and water). It is interesting to note that, for various aqueous organic glasses, k_{GT} is greater than 1 [19,22]. The very low T_g of water and the curvature of the dependence of T_g on water content indicate that, in the low water-content region, trace amounts of water will produce a marked depression of T_g, while the effect is less marked at high water contents (see Figs. 1, 2) [2]. This plasticizing effect is more marked, the greater the k_{GT} value. In this way, the k_{GT} value is an index of the plasticizing, T_g-depressing effect of water at low water contents.

k_{GT} values, calculated from T_g curves for several fruits, are very similar to those for sucrose-containing systems. Telis and Sobral [124,125,190] have observed that the T_g values for various dehydrated fruits are mainly determined by the sucrose present.

Several alternatives for the Gordon–Taylor equation (such as Couchman–Karatz–Kwei) have been discussed by Corti et al. [29].

Roos [152] reported that the k_{GT} values for various sugars could be related to their anhydrous T_g values. A linear relationship between k_{GT} and T_g was then used to derive k_{GT} values for various carbohydrates [29,152], which can be useful for predictive purposes, as an empirical parameter.

From analysis of T_g vs. a_w curves, a linear relationship was found between 0.12 and 0.65 a_w, but outside this range, nonlinearity was observed. Various authors have proposed a third-degree polynomial equation for describing the dependence of T_g values on a_w, including the nonlinearity in the very dry and wet regions [75]. This type of equation was considered useful for estimating the T_g for any form of milk (powder or concentrate with any fat content and any degree of lactose crystallization).

5.3 The w_g', T_g' point

The solute concentration of the maximally freeze-concentrated unfrozen matrix (w_g'), and its water content can be calculated from the corresponding T_g' value, by applying the Gordon–Taylor equation, or derived from a state diagram based on T_g data at various water contents [1,2,8,15,191]. Thus, the water and solid contents corresponding to the T_g of the maximally freeze-concentrated matrix can give the most accurate estimate for the composition of the unfrozen, maximally freeze-concentrated phase.

Experimental analysis of the maximally cryoconcentrated matrix can be performed by a sequence of DSC runs [20]. Basically, in a first run on a diluted sample, T_g of the system, an exothermal transition for ice, indicating water crystallization (devitrification), and an endothermal peak for water melting can be observed. After the first exothermal peak, the matrix becomes cryoconcentrated, and eventually, a second T_g can be observed, which depends on scanning rate, and which corresponds to T_g' of the concentrated matrix. If the sample is allowed to remain at a temperature close to that for maximum ice formation (first exothermal peak), water has appropriate conditions for crystallizing (at an annealing temperature).

An alternative is to plot the melting enthalpy of ice, in solutions with various initial water contents, against the mass fraction of water, which shows a linear relationship [20,192]. The mass fraction of unfrozen water associated with the maximally cryoconcentrated matrix can be estimated from such

a curve by extrapolation to the abscissa at the origin ($\Delta_{fus}H = 0$ J g^{-1} when the matrix is maximally cryoconcentrated).

By another approach, the water contents of annealed samples can be determined by estimating the solute concentration corresponding to the T_g at a corresponding annealing temperature [193]. After rapid cooling of samples to –100 °C, a first DSC scan was performed, in order to detect ice-crystallization and -melting transitions. Samples were then annealed for 15 min at the onset temperature of the ice-crystallization peak observed in the first scan, and for 30 min at the end temperature of ice crystallization. After these annealing cycles, the samples were rapidly cooled down to –100 °C and then rescanned by DSC. The T_g values obtained were close to the T_g' values and in good agreement with previously published data. The corresponding w_g' values, determined after this annealing procedure, were close to those for the maximally cryoconcentrated matrices.

Many studies have reported that the solute concentrations in maximally freeze-concentrated carbohydrate matrices correspond to w_2 close to 0.8, and the dependence of T_g on experimental conditions such as solids concentration, annealing time, annealing temperature, and cooling rate have been studied in detail [2,14,17,53,152]. Because of the kinetic constraints on ice formation, solutions with high initial solute concentrations (w_2 from 0.60 to 0.8) may require several days or even weeks of annealing at T_g' < T < T_m', before the maximally freeze-concentrated state can be achieved [2,14,20].

5.4 Dynamic changes in the supercooled region

Perhaps the analysis of molecular mobility in the supercooled region of the phase/state diagrams represents one of the main challenges for the prediction and control of the rates of potential physico-chemical changes in several systems. As mentioned in Section 2.1, when the system is at conditions located between equilibrium and non-equilibrium curves of the supplemented phase diagrams, some mathematical approaches allow us to establish kinetic considerations of specific phenomena. At a given composition, the temperature range limited by T_g (or T_m' in cryoconcentrated systems) and the equilibrium curves (ice-melting and solids solubility), corresponds to conditions where molecular mobility represents a kinetic impediment of enough significance as to affect the observed order of the reactions. Diffusion-limited relaxation processes may occur above the glass transition with a rate dependent on the difference between storage temperature (T) and the glass-transition temperature (T_g) [1–22]. The location of a given system in a phase/state diagram will greatly define its molecular mobility, and, thus, may help to predict the rates of those relaxation processes. Considering the non-equilibrium nature of most of the studied systems in the present report, under processing and storage conditions, those predictions have paramount practical importance. As discussed in Section 3, the dynamic behavior of supersaturated or supercooled aqueous solutions has important implications to technological processes. Although the properties of such solutions are difficult to access experimentally in the glass-transition region [194], several mathematical approaches have been developed to describe them in the proximities of T_g. In particular, there has been increasing interest in diffusion and relaxation phenomena in the supercooled and glassy states of food and pharmaceutical systems and components, due to their influence on processing, storage, and handling [2,21,195–198]. The primary property that describes mechanical relaxation of mobile components is viscosity (η). The simplest equation describing the temperature dependence of viscosity is the Arrhenius equation

$$\eta = \eta_o e^{-(\frac{E_a}{RT})} \tag{3}$$

where η_o is a constant, R is the gas constant, and E_a is an energy barrier to flow. Sugar–water systems show a departure from this model in the proximity of T_g, and therefore they have been classified as "fragile" glass-forming liquids [194]. The deviations from Arrhenius behavior may be accounted for by

several semi-empirical models, such as WLF [68], Vogel–Tamman–Fulcher (VTF) [194,199], and Power Law [200].

The WLF equation [68,69] relates the η at T to the η_g at T_g, as a function of the difference between T and T_g, as follows:

$$\log \frac{\eta}{\eta_g} = \frac{c_1 (T - T_g)}{c_2 + (T - T_g)} \tag{4}$$

As discussed in Sections 2.2 and 2.4, in a cryoconcentrated system, T_m' represents the "mobility temperature" at which the constrains due to solute mobility are overcome during warming. It represents the temperature at which the diffusion of solute in the maximally freeze-concentrated system can occur in a practical experimental time frame, and is an appropriate reference temperature (instead of T_g) to use in the WLF equation in this kind of systems for estimating solute diffusion and reaction rates at sub-freezing temperatures above T_m' [201]. The VTF equation for viscosity can be expressed as follows:

$$\eta = \eta_\infty e^{\left(\frac{B}{T - T_o} \right)} \tag{5}$$

where η is the viscosity at infinite temperature, and T_o is the temperature at which the relaxation time relevant to molecular displacements becomes infinite. The value of T_o estimated for aqueous sugar systems, from data reported by Parker and Ring [196], was 184 K. Constant B can be calculated as the slope of the linearized form of the VTF equation.

Alternatively, Hill and Dissado [200] formulated a Power Law description of relaxation (eq. 6):

$$\eta = \kappa (T - T_g)^{-m} \tag{6}$$

where κ and m are constants.

The WLF equation has been frequently applied in polymer science, using T_g as a reference temperature and fixed constants (C_1 and C_2) obtained by averaging values for many different polymers [172]. The VTF and WLF equations are interconvertible, but Angell et al. [194] have suggested that, in sugar systems, the VTF is conceptually better than the WLF form, because the VTF has coefficients that can be considered to be of more universal applicability.

The WLF equation has the advantage that its reference temperature, T_g, can be determined experimentally. However, determination of viscosity close to T_g is difficult to access experimentally, because it is extremely high (e.g., $\eta_g = 10^{15}$ mPa s). It can thus be necessary to define another reference temperature within an experimentally accessible range. In this way, in systems for which η_g is unknown and cannot be reliably measured, use of another reference temperature can be convenient [202,203].

There have been several studies on the viscosity–temperature relationship in aqueous sugar solutions, or in amorphous sugar phases in partially frozen systems, and have compared viscosities experimentally determined and predicted by different models [197,204–206]. Longinotti and Corti [204] performed a comprehensive analysis of the different theoretical and semiempirical models to deal with viscosity in the supercooled regime. Equations 3 to 6 have also been used to analyze the temperature dependence of diffusion-limited relaxation processes, such as sugar crystallization and chemical reaction rates [57,86,96]. In such cases, η can be replaced by $1/k$ in eqs. 3 to 6, where k represents the variable dynamic property under study (crystallization or any other reaction rate), which is directly proportional to molecular mobility and inversely proportional to viscosity.

Generally, all the above models can be employed quite satisfactorily to describe experimental behavior at temperatures far above T_g. However, no extrapolation is possible from the particular temperature range for which the model coefficients were calculated. For viscosity and sugar crystallization data [96,206], the Arrhenius model predicted a smaller temperature dependence, while the WLF equation predicted a greater temperature dependence close to T_g (Figs. 9a,b). The application of these equations to describe the behavior of an enzyme denatuarion is shown in Fig. 9c.
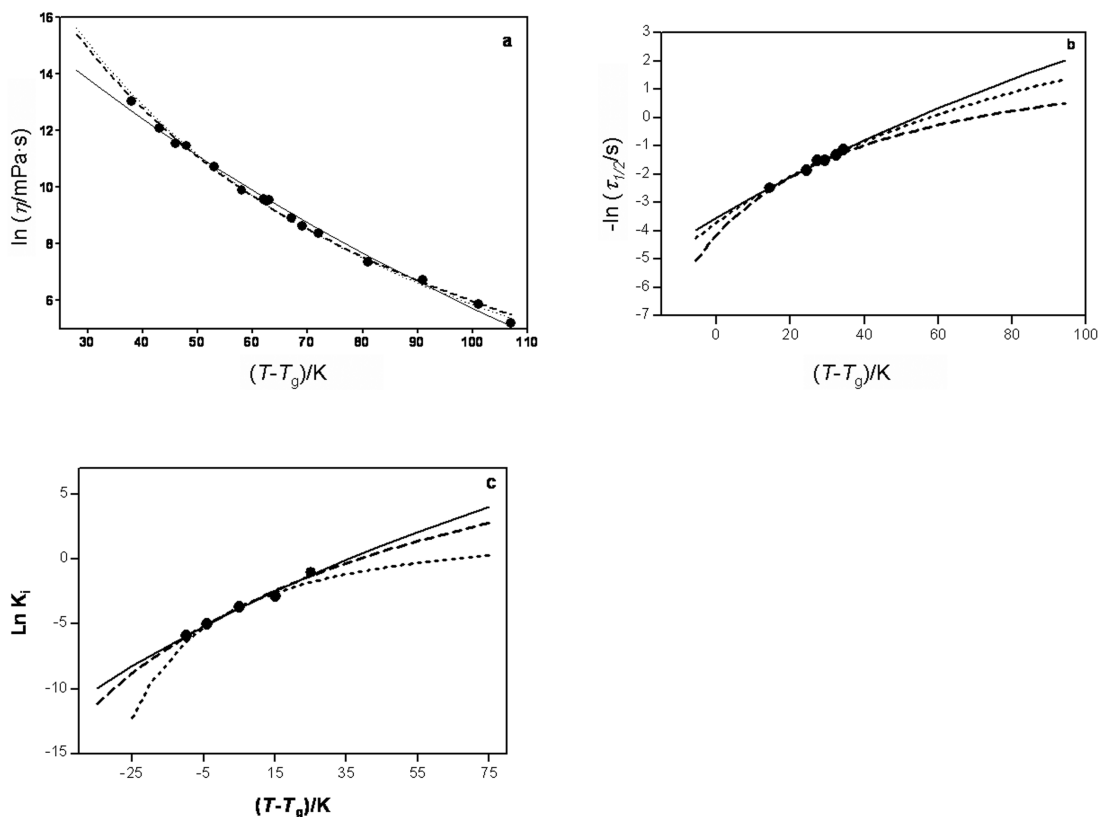
Fig. 9 Examples of the application of the Arrhenius (—), WLF (·····), and VTF (---) equations for describing: (a) dependence of honey viscosity (η), data from ref. [205]; (b) time for lactose crystallization ($\tau_{1/2}$) at water activity (a_w) 0.33, data from ref. [81]; (c) lactase inactivation rate (K_i) in an amorphous poly(vinyl)pyrrolidone (PVP) matrix at $a_w = 0.3$, data from ref. [96] as a function of the temperature difference to the glass-transition temperature ($T–T_g$).

5.4.1 Sugar crystallization

Crystallization in the glassy state below T_g is kinetically inhibited. It is initiated concurrently as increasing temperature or water content above T_g with the concomitant structural changes showing an increasing rate with increasing $T–T_g$ [2,13,15]. Crystallization of solutes may also occur in partially freeze-concentrated matrices [19], since these solutions are done only to the freeze-concentrated rubbery state where lactose is almost insoluble.

    There are several different methods available for studying the crystallization of amorphous sugars [18,75,96]:

- Crystallization kinetics at constant relative humidity can be investigated by monitoring time-dependent changes in sorbed water contents during storage and observed differences resulting from crystallization [88,207–211].
- Measurements of the different amounts of heat released by crystallization, as determined by isothermal and non-isothermal DSC [19,87].
- Analysis of the increasing intensities and areas of peaks in X-ray diffraction (XRD) patterns is also possible [143,212]. XRD is a practical technique for identifying crystal forms and for following or characterizing rates of crystallization of components, especially when systems are complicated, such as systems with several crystallizing components.
- Microscopy and infrared and Raman spectroscopies have also been used to study the crystallization of amorphous systems [87].

5.4.2 Crystallization kinetics

The extent of crystallization, α, can be calculated from the melting enthalpy in a dynamic DSC run, from the ratio of the endothermic melting peak area for a given sample and the calorimetric enthalpy of melting for the corresponding pure substance (eq. 7):

$$\alpha_{M} = \frac{\Delta_{fus}H}{\Delta_{fus}H^{*}} \tag{7}$$

where α_{M} denotes the crystallization degree obtained from the melting enthalpy; $\Delta_{fus}H$ is the specific enthalpy of melting of the solute in a given sample; and $\Delta_{fus}H^{*}$ is the specific enthalpy of melting of the pure solute. This approach has been employed to calculate the degree of trehalose crystallization [92], or the degree of retrograded (or recrystallized) starch after storage [214].

    Alternatively, the degree of crystallinity, or relative amount of material crystallized, can be determined from isothermal DSC runs by integration of the exothermal crystallization peaks [86], to obtain the heat of crystallization at specified time periods (eq. 8):

$$\alpha_{C} = \frac{\Delta Q_{ct}}{\Delta Q_{c}} \tag{8}$$

where α_{C} denotes the crystallization degree obtained from the heat involved in solute crystallization; ΔQ_{ct} represents the heat of crystallization exchanged at time t (which is proportional to the exothermal area in the DSC thermogram) and ΔQ_{c} corresponds to the total heat of crystallization, obtained from the area under the entire crystallization curve ($\alpha_{c}=1$ corresponds to the total peak area).

    It has to be pointed out that if the DSC run is performed at adequately low rates, the melting fenomenon procceeds quite close to the equilibrium conditions, while crystallization occurs in non-equilibrium conditions.

    The Johnson–Mehl–Avrami–Komogorov (JMAK) equation [215–217] can be employed to investigate the kinetics of crystallization, by fitting the degree of crystallinity against time t, as follows (eq. 9):

$$1 - \alpha = e^{-K_{c}t^{n}} \tag{9}$$

where K_{c} is the rate constant for isothermal crystallization, which depends primarily on crystallization temperature, and n is known as the Avrami index, a parameter characteristic of nucleation and growth mechanisms for crystals, related to the number of dimensions in which crystal growth takes place. The height and width of exothermal peaks, and the enthalpy involved, are the representative parameters of the crystallization process. The parameters K_{c} and n can be obtained from experimental data. The

numerical value of K_c is directly related to the overall rate of crystallization, and is a strong function of temperature. Reciprocal crystallization half-time values ($\tau_{1/2}$) can be calculated using the following equation (eq. 10):

$$\tau_{1/2} - = -\ln\left(\frac{0.5}{k}\right)^{\frac{1}{n}} \tag{10}$$

Equation 10 is particularly valuable because it can provide important information about a crystallization mechanism [210]. For example, crystallization kinetics of synthetic polymers are often modelled using the Avrami equation [215], as reviewed by Sperling [172]. Crystallization in starch-containing foods is often referred to with the term retrogradation, which is time-dependent and has been suggested to be kinetically controlled by the glass transition of starch [2]. The Avrami equation has been successfully fitted to kinetic crystallization data for lactose [88,211]; trehalose and sucrose [92] and starch gels [209,212,217,218]. The value of the Avrami exponent, *n*, was found to be higher at lower storage temperatures and at conditions with small T–T_g values.

Jouppila et al. [210] and Vuataz [75] described the time needed for lactose crystallization (from 3 min to 1 day), through the WLF equation [68]. Using sets of data for isothermal storage of whole milk at different temperatures between 303 and 383 K, the WLF model gave very good approximations for the time to lactose crystallization.

Different additives may affect the molecular mobility of amorphous lactose and consequently its crystallization rate [210,213]. The effect of a mixture of several sugars on crystallization and stability of embedded enzymes has been analyzed in freeze-dried model systems. In amorphous trehalose–lactose systems, the time to crystallization of lactose increased in the presence of trehalose [86]. The onset temperatures for trehalose or sucrose crystallization, determined by DSC, increased in the presence of raffinose or lactose, and crystallization was entirely avoided during the DSC run, if enough of the second sugar was present [86].

Buera et al. [74] showed that the presence of proteins retarded sugar crystallization, and in parallel, sugars retarded protein denaturation. Mazzobre et al. [83] have also reported the inhibition of trehalose crystallization, due to the presence of polymers or salts. Because of this, when simple sugar or polyol matrices are designed for protecting biomolecules, which is a common practice in pharmaceutical or food-ingredient formulations, the addition of a second excipient can be beneficial (see Section 4.2).

5.5 Water and solids molecular dynamics using time-domain NMR

As discussed in Section 5.1, time-resolved ^{1}H-NMR can be used as a complementary or alternative technique to DSC, to determine T_g. In addition, ^{1}H-NMR relaxation times provide a better understanding of water and food-solids mobility in complex and heterogeneous systems [208,220–222]. Water-molecule mobility can be analyzed by NMR spectroscopy, using proton (^{1}H), deuterium (^{2}H), and oxygen-17 (^{17}O) nuclei. The ^{1}H nucleus is the most abundant NMR-detectable species, and with a spin quantum number (I) of 1, its signal acquisition is relatively easy. Since relaxation times from μs up to seconds can be analyzed, a wide range of molecular mobilities can be distinguished, covering all the regions of the phase/state diagram.

Characterization of the dynamics of starch polymers and water is one of the most established and prolific areas of the application of NMR to starch-based foods [184].

As a consequence of their association with molecular mobility, the slopes of T_2 obtained by free induction decay (T_{2FID}) vs. temperature curves below T_g have been related to rates of product quality changes during storage [183]. A non-zero slope in a plot of T_{2FID} vs temperature at $T < T_g$ has been suggested to indicate that some mobility exists, even before a glass transition occurs [183].

The spin-spin relaxation time, T_2, evaluated using a Hahn spin-echo sequence, allows one to measure proton magnetic relaxations characterized by higher T_2 values (longer relaxation times, corresponding to more mobile protons) than those determined by FID. In the Hahn spin-echo pulse sequence, a refocus 180º pulse is employed, and an interpulse time (τ) elapses between 90º and 180º pulses (90º-τ-180º), for which a range is selected to allow registration of the complete decay of the signal. The decay envelopes after a Hahn sequence are typically fitted to bi-exponential behavior. In this way, the spin-echo pulse sequence can be used to differentiate proton populations with different mobilities, as a function of water content, and to study the relaxation of water protons, after the protons corresponding to solids have relaxed. Short relaxation times, can be attributed to solids and water molecules displaying strong interactions with solids, and are close to T_{2FID} values. The longer relaxation times correspond to proton populations with higher mobility and therefore weaker interactions with solids.

As water content increases, increasing relaxation times can be related to more mobile proton populations [104,105]. The intensity of an NMR signal corresponding to a particular proton population offers a relative estimation of the number of protons contributing to given T_2 values. The signal intensity of water protons with higher mobility increases as increasing water content, indicating the increased number of water molecules contributing to it [104,105,223]. Partanen et al. [224] observed a decrease in molecular motion in amylose films, induced by glycerol, and evidenced by longer relaxation times at temperatures below T_g. This effect was related to an antiplasticizing effect of glycerol, relative to that of water [2], but with a further water- or glycerol-content increase, a plasticizing effect became evident [224].

6. NON-EQUILIBRIUM PHASE TRANSITIONS AND LIVING ORGANISMS

While most living organisms survive within a narrow range of environmental conditions, some others can survive under extreme stresses, by adapting to situations that would otherwise be lethal. They develop various strategies for protection against extreme temperatures and dehydration, which enable them to survive conditions such as lack of water (cryptobiosis or anhydrobiosis) and freezing temperatures (cryobiosis) [49–51,225].

Since such tolerant living organisms face the same problems with protecting their important biomolecules, as pertain to food and pharmaceutical preservation, by studying the strategies used in nature, one can develop innovative procedures for use in food and pharmaceutical technologies [226].

The strategies employed by tolerant organisms for avoiding injuries caused by dehydration and freezing, can be interpreted and analyzed with the help of simplified temperature-composition state diagrams, such as that schematized in Fig. 10, generically designed from an approximation to the composition of cell cytosol, which is similar to those compositions also found for seeds and various biological tissues [10,89,176,227].

6.1 Anhydrobiotic organisms

Glass formation is a natural mechanism for the preservation of complex anhydrobiotic organisms, which can tolerate desiccation and survive for extended periods in a dry state [26,227,228]. In response to dehydration, the cytoplasm of desiccation-tolerant organisms forms glasses that contain large amounts of soluble non-reducing sugars, and their state diagrams resemble those of simple sugar mixtures (see Fig. 10). Crowe et al. [26] reported that, although vitrification of structure is necessary to improve enzyme stability, it is not the only condition that characterizes protective molecules, since specific hydrogen-bond interactions between matrix and protein are also thought to be needed. As direct interaction of sugars with protein molecules that are imbedded in a glassy matrix is believed to prevent protein denaturation and lead to optimal preservation [24], it is important that a sugar remain in a non-crystalline state, which could be either glassy or supercooled. It is to be noted that, when solute crystallization occurs, the composition of the non-crystalline phase changes, and often a resulting increase
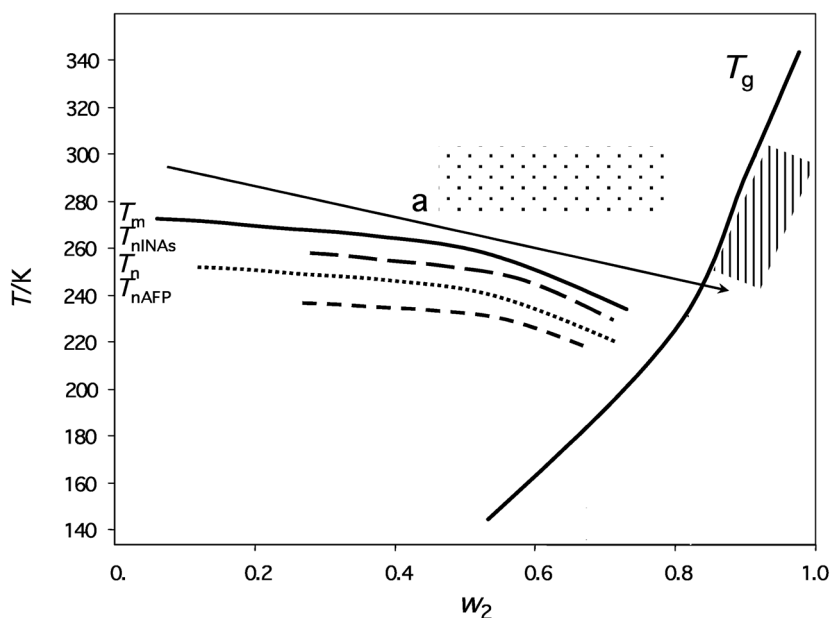
Fig. 10 State diagram showing the conditions and mechanisms at which some living organisms develop strategies which allow them to survive adverse conditions.

▨ Conditions under the glass-transition temperature (T_g) curve suitable for anhydrobiotes conservation.

⊡ Potential conditions allowing survival of the recalcitrant seeds.

T_m: equilibrium temperature of ice crystallization; T_n homogeneous ice-nucleation temperature; T_{nINAS} modified ice-nucleation temperature by INAs; T_{nAFP}: modified ice-nucleation temperature by AFPs. Line a indicates the conditions under protective dehydration.

in deteriorative reaction rates is observed [74]. Organisms that are anhydrobiotic by nature, such as *Saccharomyces cerevisiae* and tardigrades, have been found to accumulate up to 20 % of their dry weight of α,α-trehalose and to undergo vitrification upon drying [25]. Pollen, seeds, and resurrection plants (such as *Selaginella lepidophyl*) accumulate sucrose and other non-reducing β-furanosides such as raffinose, stachyose, or verbascose. Desiccation-tolerant plants use the disaccharide sucrose, for this purpose [25]. In the cases of seeds, embryos, and plant tissues, the presence of several oligosaccharides has been related to seed longevity, due to their protection of proteins and membranes, and to their prevention of sucrose crystallization [229,230]. Dried yeast cells have been reported to have T_g values and water-sorption isotherms that are independent of the amount of trehalose naturally present. However, their viability is dramatically dependent on the quantity of this disaccharide present [231]. Besides sugars, proteins (dehydrines), salts, and amino acids are accumulated by organisms resistant to dehydration, and act in different ways, stabilizing proteins and membranes, contributing to osmotic adjustment, or as free-radical scavengers.

Vitrification of protective sugars is perhaps the main strategy in nature to avoid the crystallization of sugars in anhydrobiotic organisms.

The influence of different yeast (*S. cerevisiae*) cellular fractions has been studied, in an attempt to gain knowledge on the feasibility of trehalose crystallization in yeast cells. Certain constituents of *S. cerevisiae* cells inhibited/delayed trehalose crystallization upon humidification at high relative humidities [89]. This revealed that cellular structures naturally possess components that act to delay or inhibit sugar crystallization in the interior of the cells. Although crystallization of sugars in the cytoplasm has been assumed to be a cause of viability loss, sugar crystallization is most of the times difficult to detect in cells or tissues due to the interfering effect of the accompaning solutes [175,227].

6.2 The problem of recalcitrant seeds

The cytoplasmic glass in seeds is composed mainly of sugars (sucrose and oligosaccharides comprise about 10–20 % of the dry weight), high-molecular-weight oligosaccharides, and proteins. Vitrification of cytoplasm components in orthodox seeds has been proposed to be advantageous for germplasm stability, and component transitions may affect seed viability [232]. As storage temperature or water content increases, seeds can undergo a glass-to-liquid transition (at T_g), resulting in an increase in molecular mobility. Whether or not seed tissues are in a glassy state can depend on both seed water content and storage temperature. In orthodox seeds, glass formation as water content is depressed is thought to limit deteriorative reactions [230]. However, desiccation-sensitive organisms, such as recalcitrant seeds, generally lose their viability during drying, at water contents at which the glassy state has not yet been achieved [227]. The location of potential conditions allowing survival of the recalcitrant seeds is shown in Fig. 10.

Recalcitrant seeds (e.g., *Araucaria angustifolia*, palm) do not tolerate a reduction in water content below a relatively high level, without loss of viability, and a glass cannot be formed [229,232]. Conventional storage techniques are thus not applicable to such seeds, and cryopreservation is the only feasible alternative for their long-term storage [231]. Panza et al. [233] have observed that, at water contents (or relative humidities) at which the embryos of recalcitrant *A. angustifolia* seeds retain their viability (at and above a_w 0.85), water freezes upon cooling to subzero temperatures. Since the high freezable-water content of such seeds can promote injuries, their preservation at low temperatures represents a challenge in germplasm banks. Thus, recalcitrant seeds are good models for analyzing the impact of freezing rate, storage time, and temperature on the degree of injury. If certain plant tissues undego a rapid cooling (e.g., to 77 K), only minor damage occurs [233]. Those seeds with lower contents of freezable water would be more easily cryopreserved [230]. The preservation of recalcitrant seeds could be improved by vitrification, either by dehydration, after imbibition of the embryos with protecting agents, or by cooling while avoiding ice formation, but this is an area that requires further research, and would be of interest for biodiversity preservation in germplasm banks.

Sacandé et al. [234] have studied the phase and state transitions in tropical neem seed (having low tolerance to dessication), as affected by water. Their results indicated that, through the use of phase/state diagrams, a better insight could be obtained into the peculiar behavior of dry neem seeds, allowing the development of efficient methods for storage of tropical seeds displaying intermediate storage stability.

6.3 Survival in frozen environments

Intracellular ice formation can change the chemical environment of a biomolecule. In particular, pH changes and ionic-strength increases may damage proteins and nucleic acids [43]. In a related vein, injuries due to mechanical changes can affect such systems; large ice crystals can disrupt tissue structures, so control of ice-crystal growth can be important to the survival of organisms in winter. Some plants and animals have evolved means to prevent the lethal effects of ice crystals forming in their cells. The mechanisms by which certain organisms survive extreme low temperatures are schematized in Fig. 10, and they include: extracellular water crystallization (formation of ice crystals outside cell membrane), use of antifreeze proteins (AFPs), and glass formation [235].

In freeze-tolerant species, proteinaceous ice nucleators agents (INAs) trigger extracellular freezing at high subzero temperatures, either to provide protection from cold by released heat of fusion, or to establish a protective (extracellular) freezing that drives water out of cells, thus decreasing the temperature at which intracellular ice could form [235]. The amino acids within INAs are thought to form templates for ice, which can serve as embryos for ice formation [236]. Among the most efficient INAs in nature are ice-nucleating proteins found on the surface of certain bacteria, such as *Pseudomonas syringae*, *Erwinia herbicola*, and *Pseudomonas fluorescens*, commonly found on plant leaves and other above-ground plant parts [237].

In contrast, some organisms will die if they freeze, so they need to avoid freezing by maintaining their body fluids in a liquid state, even at extremely low subzero temperatures. Certain freeze-avoiding species increase their supercooling potential by removing ice nucleators and accumulating polyols [237]. Fish, insects, and some plants that live in Arctic and Antarctic regions have evolved to produce AFPs, which inhibit the growth of ice crystals by adsorption to ice surfaces [237]. Another class of non-freezing-tolerant organisms, such as the Arctic springtail, *Onychiurus arcticus,* and some insects, use a strategy of protective dehydration [235]. In protective dehydration (Fig. 10), loss of water occurs across a diffusion gradient between an organism's supercooled cell fluids and ice in its surroundings, such that the extent of freezing-point depression always exceeds the environmental temperature, and eventually, the organism loses sufficient water and desiccates, to ensure that a freezing event cannot occur. Parallel to the induction of extensive dehydration, rapid synthesis and accumulation of the membrane/protein cryoprotectant, trehalose, and some other low-molecular-weight compounds occur. As a result, the water in cells cannot freeze above –40 °C [235].

AFPs and antifreeze glycoproteins (AFGPs) were first identified in the 1970s in Antarctic fishes that can survive in seawater that is colder than the freezing temperature of their blood, but such AFPs and AFGPs were later also found in various microorganisms, insects, plants, and nematodes [237]. Although such proteins were first thought to act via a colligative effect, by decreasing the meting point of water, it was later observed that they act by preventing the growth of ice crystals, having only a small effect on colligative properties [237]. The ability to modify the rate and shape of ice-crystal growth and protect cellular membranes during lipid-phase transitions has resulted in identification of a number of potential applications of AFGPs as food additives, and in applications for the cryopreservation and hypothermal storage of cells and tissues [238,239].

The efficiency of freezing and the resulting quality of commercial products are affected by two important factors: supercooling (the cooling of liquid below its freezing point, without freezing) and nucleation (the initiation of the crystallization of liquid water into solid ice). Both phenomena can be modified by the presence of two kinds of proteins that show opposite behaviors [238], both of which provide enormous technological potential in industrial processes [41].

INAs, on the one hand, decrease the extent of supercooling and so increase the temperature of heterogeneous nucleation (T_{nINAS} in Fig. 10), thus decreasing the freezing time and promoting the formation of a large number of ice crystals with dendritic structure [235]. AFPs, on the other hand, decrease the temperature of heterogeneous (T_{nAFP} in Fig. 10) supercooling, generate very small ice crystals, lower the freezing temperature, and retard ice recrystallization on frozen storage [237]. Major potential applications of INAs and AFPs have been reviewed elsewhere [41,238]. Beneficial effects of INAs would be manifested in reduced energy costs and smaller ice-crystal sizes, the latter favoring quality and shelf-life improvements. Bacterial INAs have been employed in freezing processes for meats [240] and products difficult to concentrate or freeze-dry, such as fruit juices or pastes [241]. The management of ice-nucleation and -crystallization times can also be employed in the development of new products [242]. AFPs are natural products that constitute part of a normal diet, through their occurrence at high concentrations in food fishes and vegetables. AFPs from vegetables have a number of potential applications. For example, they have been shown to improve the texture of frozen dough and the retention of volatile compounds in crumb foods, through the addition of a concentrated carrot extract containing carrot AFP [243].

Table 7 summarizes the main strategies discussed in Section 6, which allow some living organisms to survive adverse conditions, in relation to their location in a state diagram.

Table 7 Main strategies which allow some living organisms to survive adverse conditions, involved mechanisms and representative examples of each group [235–237].

System	Survival mechanisms	Action	Involved solutes	Examples
Anhydrobiotes	Glass formation at low water content	Reduce molecular mobility, hydrogen bond interactions	Non-reducing sugars (trehalose, sucrose, raffinose, stachyose) Proteins: dehydrines	*Artemia salina*, yeast cells, tardigrades, flatworm, insects larvae, rotifers; resurrection plants pollen, orthodox seeds
Freezing-tolerant	Promote extracellular water crystallization	Increase ice nucleation temperature, decrease freezing time	Adaptative INAs	Insects, arthropods or springtails (snow flea), vertebrates (hatchling painted turtles)
Freezing-avoiding	Inhibit ice crystals growth	Increase ice nucleation temperature	AFPs (non-colligative effect)	Polar marine fishes, terrestrial invertebrates, insects, artropodes, nematodes, plants, fungi
	Inactivation of ubiquos INAs	Inhibit ice nucleus formation by a foreign particle	Proteins, polymers	Antarctic bacteria (*Pseudomonas fluorescens*)
	Vitrification at high water content	Reduce molecular mobility	Low-molecular-weight compounds, polyols	Freshwater snail (*P. canaliculata*); fly (*Eurosta solidaginis*); frog (*Rana sylvatica*)

7. FUTURE PROSPECTS

Liquid–solid nucleation of a supercooled aqueous solution may appear to be a simple phenomenon, but it remains a poorly understood process of evolution from a metastable state to a final equilibrium state. Input from fundamental research in this area is needed [243]. Carefully designed experiments to measure temperatures and times for nucleation and crystal growth need to be developed [37,244].

Studies of the delay/inhibition of sugar crystallization in supercooled liquids at low water contents may increase the range of applications of sugars as excipients for food-ingredient and pharmaceutical formulations for specific purposes.

The presence of ice surfaces has been identified as a cause of freeze-induced perturbations of the folding of native proteins, but these interactions are poorly understood. Gabellieri and Stambrini [245] have reported that a binding method using a fluorescent probe may find practical utility in testing the effectiveness of various additives employed in frozen or freeze-dried protein formulations. Future research work in this area could be helpful in the development of "ice-managing" additives.

Currently, relatively long-term storage of living cells in a high-water-content range can be done only in cryoprotectant solutions at extremely low subzero temperatures, and much of the time, media formulations are developed on an empirical basis [243,244]. A standardized, scientifically based vitrification protocol for cryopreservation has yet to be defined, one that takes into account the many variables that can profoundly influence its effectiveness and its potential to improve the survival rates of vitrified cells: e.g., type and concentration of cryoprotectant; temperature of the vitrification solution at

exposure; duration of exposure to the final cryoprotectant, before plunging the material into liquid nitrogen.

The relatively high cost of freezing processes currently used in the food industry, and the search for products with special structures, could represent a major impetus to innovations in freezing techniques (e.g., wider use of INAs or AFPs). Additional work to analyze costs vs. benefits, balancing energy savings and product-quality improvements, is essential, prior to final commercialization or industrial applications [41].

Potential areas for further research include the study of macroscopic and molecular properties of materials, such as the incidence and effect of sub-T_g relaxations on the kinetics of chemical reactions, and of local heterogeneities in water distribution at microscopic length scales. Also, quantification of structural effects, such as collapse and compression, would be valuable for a more complete interpretation of the kinetics of deteriorative reactions.

In relation to analytical tools, developments in infrared thermography, different microscopic techniques, and magnetic resonance spectroscopies and imaging techniques, for cryo- and dehydro-preserved systems, have been shown to be powerful tools for the interpretation of the mechanisms of dynamic changes in metastable systems, and are expected to contribute further, with new advances in these areas [245,246].

8. CONCLUDING REMARKS

A major advantage from constructing supplemented phase/state diagrams is in identifying the different states and transitions of a material, such as freezing point and glass transition, which aids understanding of the complex changes that potentially will occur, when water content and temperature are varied [2]. A state diagram also assists one in identifying conditions necessary for storage stability, as well as in selecting suitable conditions of temperature and moisture content for processing [2,146,245]. Analysis of a phase/state diagram is recommended, before significant modifications in formulation and handling procedures are made in advance of large-scale food production.

We have analyzed the rates of different physico-chemical phenomena, from the perspective of phase/state diagrams for the matrices in which they take place. In order to optimize the efficiency of dehydro-protectant agents for biomolecules, construction of state diagrams is a good starting point for analysis of the dynamics of quality changes, but such diagrams should be complemented by knowledge about any intermolecular interactions that may take place. Beyond supramolecular aspects, such as T_g and crystallinity, the density of molecular packing of matrices, reducing power, and hydrogen-bonding capacity can also contribute to determining the effectiveness of biomolecule protectants. Electrolytes commonly present in biological media or food and pharmaceutical formulations have been shown to modify metastable systems, affecting the kinetics of water and sugar crystallization and enzyme inactivation, by both molecular and supramolecular interactions [92,203].

Real, complex systems such as foods or biological materials cannot be easily represented by a binary-state diagram. However, if the all nonaqueous components are considered as a whole (total solids content), the glass-transition and ice-melting curves can be displayed with sufficient accuracy to be of value and a pseudobinary diagram can be easily be obtained [201]. As discussed in this report, many times the dominant solute/s within a system can be identified (e.g., lactose in dairy products [75,88,123,128,129], sucrose in confectionery and baked foods, starch in cereal products, sugars in fruit, vegetable tissues including seeds). This is acceptable provided no components of the nonaqueous solute mix separates out, and proved to be an adequate approximation for analyzing the global behavior of dry and frozen foods [2,14-18,26,30,201,251], seeds, and cell preservation formulations [35,37,41,42,46-48,72,79,153,232,234]. It should be realized, however, that in complex systems different regions or different component molecules in different regions may exist, and thus may require the description by multiple binary state diagrams [201].

Glass transition alone may not be sufficient as a generic criterion for determining a system's stability, since specific solid–water interactions and other structural characteristics of systems can also exert control over the dependence of reaction rates on relative humidity [170]. In addition to affecting chemical reactions via a_w and by plasticizing amorphous systems [6], water mobility itself has been demonstrated to have a direct impact on chemical reactivity in low- and intermediate-moisture systems [104,105]. Nevertheless, glass transition is definitely one of the factors affecting system stability [2], and a future challenge remains to combine the glass-transition concept with other pertinent mechanisms or factors [247]. In such a way, beyond the valuable information provided by locating plausible system conditions (compositions/temperatures) on supplemented phase/state diagrams, structural aspects of matrices in which a reaction takes place, water-sorption properties, and mobility have also been identified as key aspects required for a more complete interpretation to describe the dynamics of major chemical reactions [104,105,119].

It is interesting to note that the different aspects discussed in the present paper illustrate synergistic interactions at the multidisciplinary interfaces of physics, chemistry, medicine, biotechnology, food science and technology, pharmacy, and biology, with regard to the preservation of living organisms such as embryos and cells, structures such as liposomes, and also labile biomolecules such as proteins, antibodies, and hormones.

MEMBERSHIP OF SPONSORING BODY

Membership of the Physical and Biophysical Chemistry Committee for the period 2008–2009 was as follows:

President: M. J. Rossi (Switzerland); *Vice President*: A. J. McQuillan (New Zealand); *Secretary*: R. M. Lynden-Bell (UK); *Titular Members*: J. H. Dymond (UK); A. Goldbeter (Belgium); J.-G. Hou (China); R. Marquardt (France); B. D. Sykes (Canada); K. Yamanouchi (Japan); *Associate Members*: A. R. H. Goodwin (USA); S.-J. Kim (Korea); G. R. Moore (UK); C. Prestidge (Australia); M. Rico (Spain); A. K. Wilson (USA); *National Representatives*: F. Akhtar (Bangladesh); M. Chalaris (Greece); A. Friedler (Israel); O. V. Mamchenko (Ukraine); S. Riazuddin (Pakistan); S. Stølen (Norway); V. Tsakova (Bulgaria); M. Witko (Poland).

Membership of the Task Group on the Thermodynamic and Non-equilibrium Criteria for Development and Application of Supplemented Phase Diagrams was as follows:

Chair: H. R. Corti (Argentina); *Members*: C. A. Angell (USA); T. Auffret (UK); M. P. Buer (Argentina); H. Levine (USA); D. S. Reid (USA); Y. Roos (Ireland); L. Slade (USA).

ACKNOWLEDGMENTS

REFERENCES

1. L. Slade, H. Levine. *Carbohydr. Polym.* **8**, 183 (1988).
2. L. Slade, H. Levine. *Crit. Rev. Food Sci. Nutr.* **30**, 115 (1991).
3. L. Slade, H. Levine. *J. Food Eng.* **22**, 143 (1994).
4. L. Slade, H. Levine. In *Food Preservation by Moisture Control (ISOPOW Practicum II)*, G. Barbosa-Cánovas, J. Welti-Chanes (Eds.), pp. 33–132, Technomic, Lancaster, PA (1995).
5. L. Slade, H. Levine. *J. Food Eng.* **24**, 431 (1995).
6. L. Slade, H. Levine. *Adv. Food Nutr. Res.* **38**, 103 (1995).
7. L. Slade, H. Levine, J. W. Finley. In *Protein Quality and the Effects of Processing*, R. D. Phillips, J. W. Findley (Eds.), pp. 9–124, Marcel Dekker, New York (1989).

8. H. Levine, L. Slade. *Carbohydr. Polym.* **6**, 213 (1986).

9. H. Levine, L. Slade. In *Dough Rheology and Baked Product Texture*, H. Faridi, J. M. Faubion (Eds.), pp. 157–300, Van Nostrand Reinhold, New York (1990).

10. H. Levine, L. Slade. In *Physical Chemistry of Foods*, H. Schwartzberg, R. Hartel (Eds.), pp. 83–221, Marcel Dekker, New York (1992).

11. H. Levine, L. Slade. In *The Glassy State in Foods*, J. M. V. Blanshard, P. J. Lillford (Eds.), pp. 333–373, Nottingham University Press, Loughborough, UK (1993).

12. Y. H. Roos. *J. Food Sci.* **52**, 433 (1987).

13. Y. Roos, M. Karel. *Biotechnol. Prog.* **6**, 159 (1990).

14. Y. Roos, M. Karel. *Int. J. Food Sci. Technol.* **26**, 553 (1991).

15. Y. Roos, M. Karel. *J. Food Sci.* **56**, 38 (1991).

16. Y. Roos, M. Karel. *Food Technol.* **45**, 66 (1991).

17. Y. Roos, M. Karel. *J. Food Sci.* **56**, 1676 (1991).

18. Y. Roos, M. Karel. *Cryo-Lett.* **12**, 367 (1991).

19. Y. Roos, M. Karel. *J. Food Sci.* **57**, 775 (1992).

20. Y. H. Roos. In *Phase Transitions in Foods*, Academic Press, San Diego (1995).

21. Y. Roos. *J. Food Eng.* **24**, 339 (1995).

22. Y. H. Roos. In *Handbook of Food Engineering*, 2nd ed., D. Heldman, D. Lund (Eds.), pp. 288–346, CRC Press, Boca Raton (2007).

23. H. R. Costantino, S. P. Schwendeman, R. Langer, A. M. Klibanov. *Biochemistry (Moscow)* **63**, 357 (1998).

24. T. Arakawa, S. N. Timasheff. *Biochemistry* **21**, 6536 (1982).

25. J. F. Carpenter, M. J. Pikal, B. S. Chang, T. W. Randolph. *Pharm. Res.* **14**, 969 (1997).

26. J. H. Crowe, J. F. Carpenter, L. M. Crowe. *Annu. Rev. Physiol.* **60**, 73 (1998).

27. J. S. Clegg. *Comp. Biochem. Physiol., B* **128**, 613 (2001).

28. E. Shalaev, F. Franks. In *Amorphous Food and Pharmaceutical Systems*, H. Levine (Ed.), pp. 200–215, RSC Publishing, Cambridge, UK (2002).

29. H. R. Corti, C. A. Angell, T. Auffret, H. Levine, M. P. Buera, D. S. Reid, Y. H. Roos, L. Slade. *Pure Appl. Chem.* **82**, 1065 (2010).

30. D. S. Reid. In *Water Properties of Food, Pharmaceutical and Biological Materials*, M. P. Buera, J. Welti-Chanes, P. Lillford, H. R. Corti (Eds.), pp. 59–76, CRC Taylor and Francis, Boca Raton (2004).

31. F. Franks. In *Freeze-Drying of Pharmaceuticals and Biopharmaceuticals. Principles and Practice*, Chap. 5, RSC Publishing, Cambridge, UK (2007).

32. B. Luyet, D. Rasmussen. *Biodynamica* **10**, 137 (1967).

33. D. Rasmussen, B. Luyet. *Biodynamica* **10**, 319 (1969).

34. D. Simatos, M. Faure, E. Bonjour, M. Couach. *Cryobiology* **12**, 202 (1975).

35. B. Wowk, G. M. Fahy. *Cryobiology* **44**, 14 (2002).

36. A. P. MacKenzie. *Philos. Trans. R. Soc. London, Ser. B* **278**, 167 (1977).

37. N. Du, X. Y. Liu, C. L. Hew. *J. Biol. Chem.* **278**, 36000 (2003).

38. R. W. Hartel. In *Crystallization in Foods*, p. 325, Aspen, Gaithersburg, MD (2001).

39. D. S. Reid, W. Kerr, J. Hsu. *J. Food Eng.* **22**, 483 (1994).

40. H. D. Goff. *Pure Appl. Chem.* **67**, 1801 (1995).

41. P. J. Lillford, C. B. Holt. *Philos. Trans R. Soc. London, Ser. B* **357**, 945 (2002).

42. S. Kattera, C. Chen. *Int. Surg.* **91**, S55 (2006).

43. F. Franks. In *Water, A Compehensive Treatise*, Vol. 7, F. Franks (Ed.), Plenum Press, London (1982).

44. F. Franks. *Pure Appl. Chem.* **65**, 2527 (1993).

45. F. Franks. *Bio: Technology* **12**, 253 (1994).

46. F. Franks. In *Biophysics and Biochemistry at Low Temperatures*, Cambridge University Press, Cambridge, UK (1995).
47. F. Franks. *Eur. J. Pharm. Biopharm.* **45**, 221 (1998).
48. E. Shalaev, F. Franks. *Cryobiology* **33**, 14 (1996).
49. J. F. Carpenter, S. C. Hand, L. M. Crowe, J. H. Crowe. *Arch. Biochem. Biophys.* **50**, 505 (1986).
50. J. F. Carpenter, B. Martin, L. M. Crowe, J. H. Crowe. *Cryobiology* **24**, 455 (1987).
51. J. F. Carpenter, K.-I. Izutsu, T. W. Randolph. In *Freeze-Drying/Lyophilization of Pharmaceuticals and Biological Products*, L. Rey, J. C. May (Eds.), pp. 123–160, Marcel Dekker, New York (1999).
52. W. Wang. *Int. J. Pharm.* **203**, 1 (2000).
53. M. J. Izzard, S. Ablett, P. J. Lillford. In *Food Polymers, Gels and Colloids*, E. Dickinson (Ed.), pp. 289–300, RSC Publishing, Cambridge, UK (1991).
54. R. A. Talja, Y. H. Roos. *Thermochim. Acta* **380**, 109 (2001).
55. H. D. Goff, E. Verespej, D. Jermann. *Thermochim. Acta* **399**, 43 (2003).
56. M. Karel. In *Drying '91*, A. S. Mujumdar, I. Filkova (Eds.), pp. 26–35, Elsevier, Amsterdam (1991).
57. M. Karel, S. Anglea, M. P. Buera, G. Levi, Y. Roos. *Thermochim. Acta* **246**, 249 (1994).
58. R. Karmas, M. P. Buera, M. Karel. *J. Agric. Food Chem.* **40**, 873 (1992).
59. L. N. Bell, M. J. Hageman. *J. Agric. Food Chem.* **42**, 2398 (1994).
60. L. N. Bell. *Int. Food Res.* **28**, 591 (1995).
61. M. P. Buera, M. Karel. *Food Chem.* **52**, 167 (1995).
62. S. M. Lievonen, T. J. Laaksonen, Y. H. Roos. *J. Agric. Food Chem.* **46**, 2778 (1998).
63. K. Kouasi, Y. H. Roos. *J. Agric. Food Chem.* **48**, 2461 (2000).
64. L. N. Bell, K. L. White. *J. Food Sci.* **65**, 498 (2000).
65. G. W. White, S. H. Cakebread. *J. Food Technol.* **1**, 73 (1966).
66. S. Tsourouflis, J. M. Flink, M. Karel. *J. Sci. Food Agric.* **27**, 509 (1976).
67. E. C. To, J. M. Flink. *J. Food Technol.* **13**, 583 (1978).
68. M. L. Williams, R. F. Landel, J. D. Ferry. *J. Am. Chem. Soc.* **77**, 3701 (1955).
69. T. Soesanto, M. C. Williams. *J. Phys. Chem.* **85**, 3338 (1981).
70. S. S. Sablani, A. K. Shresthac, B. R. Bhandari. *J. Food Eng.* **87**, 416 (2008).
71. R. V. Tonon, A. F. Baroni, C. Brabet, O. Gibert, D. Pallet, M. D. Hubinger. *J. Food Eng.* **94**, 215 (2009).
72. G. Roudaut, D. Simatos, D. Champion, E. Contreras-Lopez, M. Le Meste. *Innovative Food Sci. Emerging Technol.* **5**, 127 (2004).
73. Y. H. Roos, K. Jouppila, B. Zielasko. *J. Therm. Anal.* **47**, 1437 (1996).
74. M. P. Buera, C. Schebor, B. Elizalde. *J. Food Eng.* **67**, 157 (2005).
75. G. Vuataz. *Lait* **82**, 485 (2002).
76. G. B. Stambrini, E. Gabellieri. *Biophys. J.* **70**, 971 (1996).
77. C. Van den Berg, D. Rose. *Arch. Biochem. Biophys.* **81**, 319 (1959).
78. S. Bakul, B. S. Bhatnagar, R. H. Bogner, M. J. Pikal. *Pharm. Dev. Technol.* **12**, 505 (2007).
79. W. Q. Sun, A. C. Leopold. *Comp. Biochem. Physiol.* **117A**, 327 (1997).
80. T. Suzuki, K. Imamura, K. Yamamoto, T. Satoh, M. Okazaki. *J. Chem. Eng. Jpn.* **30**, 609 (1997).
81. M. F. Mazzobre, J. M. Aguilera, M. P. Buera. *Carbohydr. Res.* **338**, 541 (2003).
82. M. P. Buera. In *Water Properties in Food, Health, Pharmaceutical and Biological Systems: ISOPOW 10*, D. S. Reid, T. Sajjaanantakul, P. J. Lillford, S. Charoenrein (Eds.), pp. 9–25, Wiley-Blackwell, Singapore (2010).
83. M. F. Mazzobre, P. R. Santagapita, N. Gutiérrez, M. P. Buera. In *Food Engineering: Integrated Approaches*, G. Gutiérrez, G. Barbosa-Canovas, E. Parada-Arias (Eds.), pp. 73–87, Springer, New York (2008).

84. I. J. van den Dries, D. Van Dusschoten, M. A. Hemminga, E. van der Linden. *J. Phys. Chem. B* **104**, 10126 (2000).

85. M. F. Mazzobre, M. P. Buera, J. Chirife. *Lebensm.-Wiss. Technol.* **30**, 324 (1997).

86. M. F. Mazzobre, G. Soto, J. M. Aguilera, M. P. Buera. *Food Res. Int.* **34**, 903 (2001).

87. P. Gabarra, W. Hartel. *J. Food Sci.* **63**, 523 (1998).

88. K. Jouppila, Y. H. Roos. *J. Dairy Sci.* **77**, 2907 (1994).

89. L. Espinosa, C. Schebor, M. P. Buera, S. Moreno, J. Chirife. *Cryobiology* **52**, 157 (2006).

90. K. M. Leinen, T. P. Labuza. *J. Zhejiang Univ. Sci.* **7**, 85 (2006).

91. L. A. Belcourt, T. P. Labuza *J. Food Sci.* **72**, C065 (2007).

92. M. P. Longinotti, M. F. Mazzobre, M. P. Buera, H. R. Corti. *Phys. Chem. Chem. Phys*. **4**, 533 (2002).

93. M. D. Ediger. *Annu. Rev. Phys. Chem*. **51**, 99 (2000).

94. S. Calligaris, M. C. Nicoli. *Food Chem.* **94**, 130 (2006).

95. A. Patist, H. Zoerb. *Colloids Surf., B* **40**, 107 (2005).

96. M. F. Mazzobre, G. Hough, M. P. Buera. *Food Sci. Technol. Int.* **9**, 163 (2003).

97. V. M. Monnier, A. Cerami. *Biochim. Biophys. Acta* **760**, 97 (1983).

98. J. W. Baynes, S. R. Thorpe. *Diabetes* **48**, 1 (1999).

99. A. La Rochette, I. Birlouez-Aragon, E. Silva, P. Morlière. *Biochim. Biophys. Acta* **1621**, 235 (2003).

100. T. P. Labuza, W. M. Baisier. In *Physical Chemistry of Foods*, H. G. Schwartzberg, R. W. Hartel (Eds.), pp. 595–649, Marcel Dekker, New York (1992).

101. J. E. Hodge. *J. Agric. Food Chem.* **1**, 928 (1953).

102. K. Eichner, M. Karel. *J. Agric. Food Chem.* **20**, 218 (1972).

103. S. Saltmarch, T. P. Labuza. *J. Food Sci.* **45**, 1231 (1980).

104. N. Acevedo, C. Schebor, M. P. Buera. *J. Food Eng.* **77**, 1108 (2006).

105. N. Acevedo, C. Schebor, M. P. Buera. *Food Chem.* **108**, 900 (2008).

106. E. O. Timmermann, J. Chirife. *J. Food Eng.* **13**, 171 (1991).

107. A. Pyne, C. H. Koustov, R. Suryanarayanan. *J. Pharm. Sci*. **92**, 2272 (2003).

108. Y. Shimada, Y. Roos, M. Karel. *J. Agric. Food Chem.* **39**, 637 (1991).

109. S. Labrousse, Y. Roos, M. Karel. *Sci. Aliments* **12**, 757 (1992).

110. M. Karel, J. M. Flink. *J. Agric. Food Chem.* **21**, 16 (1973).

111. M. Karel, I. Saguy. In *Water Relationships in Foods*, H. Levine, L. Slade (Eds.), pp. 157–173, Plenum Press, New York (1991).

112. Y. F. Maa, H. R. Constantino, P. A. Nguyen, C. C. Hsu. *Pharm. Dev. Technol*. **2**, 213 (1997).

113. O. O. Omatete, C. Judson King. *J. Food Technol.* **13**, 265 (1978).

114. K. Selim, M. Tsimidou, C. G. Biliaderis. *Food Chem.* **71**, 199 (2000).

115. G. S. Serris, C. G. Biliaderis. *J. Sci. Food Agric.* **81**, 691 (2001).

116. G. Levi, M. Karel. *J. Food Eng.* **24**, 1 (1995).

117. S. M. Prado, M. P. Buera, B. E. Elizalde. *J. Agric. Food Chem.* **54**, 79 (2006).

118. S. A. Desobry, F. M. Netto, T. P. Labuza. *J. Food Sci.* **62**, 1158 (1997).

119. B. E. Elizalde, L. Herrera, M. P. Buera. *J. Food Sci.* **57**, 3039 (2002).

120. N. C. Acevedo, V. Briones, M. P. Buera, J. M. Aguilera. *J. Food Eng.* **85**, 222 (2008).

121. L. Burin, K. Jouppila, Y. H. Roos, J. Kansikas, M. P. Buera. *Int. Dairy J.* **14**, 517 (2004).

122. M. Kim, M. Saltmarch, T. P. Labuza. *J. Food Process. Preserv.* **5**, 49 (1981).

123. L. Burin, K. Jouppila, Y. Roos, J. Kansikas, M. P. Buera. *J. Agric. Food Chem.* **48**, 5263 (2000).

124. V. R. N. Telis, P. J. A. Sobral. *Food Res. Int.* **35**, 435 (2002).

125. V. R. N. Telis, P. J. A. Sobral, J. Telis-Romero. *Food Sci. Technol. Int.* **12**, 181 (2006).

126. M. S. Rahman. In *Food Properties Handbook*, CRC Press, Boca Raton (1995).

127. R. J. Lloyd, X. Dong Chen, J. B. Hargreaves. *Int. J. Food Sci. Technol*. **31**, 305 (1996).

128. M. Kalichevsky, J. Blanshard, P. Tokarczuk. *Int. J. Food Sci. Technol.* **28**, 139 (1993).

129. L. Burin, G. Hough, M. P. Buera, J. Chirife. *Food Chem.* **76**, 423 (2002).
130. L. E. Chuy, T. P. Labuza. *J. Food Sci.* **59**, 43 (1994).
131. G. Spigno, D. M. De Faveri. *J. Food Eng.* **62**, 337 (2004).
132. E. D. Orford, R. Parker, S. Ring, A. C. Smith. *Int. J. Biol. Macromol.* **11**, 91 (1989).
133. R. C. Hoseney, K. Zeleznak, C. S. Lai. *Cereal Chem.* **63**, 285 (1986).
134. A. M. Cocero, J. L. Kokini. *J. Rheol.* **35**, 257 (1991).
135. M. T. Kalichevsky, J. M. V. Blanshard. *Carbohydr. Polym.* **19**, 271 (1992).
136. J. A. Gray, J. N. BeMiller. *Cereal Chem.* **81**, 278 (2004).
137. S. Hug-Iten, S. Handschin, B. Conde-Petit, F. Escher *Lebensm.-Wiss. Technol.* **32**, 255 (1999).
138. I. Toufeili, I. A. Lambert, J. L. Kokini. *Cereal Chem.* **79**, 138 (2002).
139. Y. H. Roos, M. Karel, J. L. Kokini. *Food Technol.* **50**, 95 (1996).
140. C. Biliaderis. In *Thermal Analysis of Foods*, V. Harwalkar, C. Ma (Eds.), pp. 168–220, Elsevier, London (1990).
141. P. Ribotta, A. León, M. C. Añón. *Food Res. Int.* **36**, 357 (2003).
142. P. H. Rasmussen, A. Hansen. *Lebensm.-Wiss. Technol.* **34**, 487 (2001).
143. C. Osella, H. Sánchez, M. de la Torre, C. Carrara, M. P. Buera. *Starch/Stärke* **57**, 208 (2005).
144. H. Jain, I. H. Jain. *NASA/CP*-2001-211029, pp. 169–182 (2001).
145. S.S. Sablani, M. S. Rahman, S. Al-Busaidi, N. Guizani, N. Al-Habsi, R. Al-Belushi. *Thermochim. Acta* **462**, 56 (2007).
146. S. S. Sablani, S. Kasapis, M. S. Rahman, A. Al-Jabria, N. Al-Habsi. *Food Res. Int.* **37**, 915 (2004).
147. V. Sunooj, K. Radhakrishna, J. George, A. S. Bawa. *J. Food Eng.* **91**, 347 (2009).
148. N. Chennamsetty, V. Voynov, V. Kayser, B. Helk, B. L. Trout. *Proc. Natl. Acad. Sci. USA* **106**, 11937 (2009).
149. K. Izutsu, S. Kadoya, C. Yomota, T. Kawanishi, E. Yonemochi, K. Terada. *Chem. Pharm. Bull.* **57**, 43 (2009).
150. K.-I. Izutsu, Y. Fujimaki, A. Kuwabara, N. Aoyagi. *Int. J. Pharm.* **301**, 161 (2005).
151. K.-I. Izutsu, S. Yoshioka, T. Terao. *Biotechnol. Bioeng.* **43**, 1102 (2005).
152. Y. Roos. *Carbohydr. Res.* **238**, 39 (1993).
153. W. L. J. Hinrichs, M. G. Prinsen, H. W. Frijlink. *Int. J. Pharm.* **215**, 163 (2001).
154. A. Martini, R. E. Kune, M. Crivelente, R. Artico. *J. Pharm. Sci. Technol.* **51**, 62 (1997).
155. H. J. Kim, C. H. Shin, C. W. Kim. *Biosci. Biotechnol. Biochem.* **73**, 61 (2009).
156. I. N. Yu, Milton, E. G. Groleau, D. S. Mishra, R. E. Vansickle. *J. Pharm. Sci.* **88**, 196 (1999).
157. A. Burger, J. O. Henck, S. Hetz, J. M. Rollinger, A. A. Weissnicht, H. Stottner. *J. Pharm. Sci.* **89**, 457 (2000).
158. V. I. Kett, S. Fitzpatrick, B. Cooper, D. Q. Craig. *J. Pharm. Sci.* **92**, 1919 (2003).
159. C. Telang, I. Yu, R. Suryanarayanan. *Pharm. Res.* **20**, 660 (2003).
160. M. J. Pikal, K. M. Dellerman, M. I. Roy, R. M. Riggin. *Pharm. Res.* **8**, 427 (1991).
161. K.-I. Izutsu, S. Yoshioka, T. Terao. *Pharm. Res.* **10**, 1232 (1993).
162. R. E. Johnson, C. E. Kirchhoff, H. T. Gaud. *J. Pharm. Sci.* **91**, 914 (2002).
163. T. Yoshinari, R. T. Forbes, P. York, Y. Karawahisma. *Int. J. Pharm.* **258**, 109 (2003).
164. K.-I. Izutsu, S. Yoshioka, S. Kojima. *Pharm. Res.* **11**, 995 (1994).
165. T. Randolph. *J. Pharm. Sci.* **86**, 1198 (1997).
166. A. I. Kim, M. J. Akers, S. L. Nail. *J. Pharm. Sci.* **87**, 931 (1998).
167. R. K. Cavatur, N. M. Vemuri, A. Pyne, Z. Chrzan, D. Toledo-Velasquez. *Pharm. Res.* **19**, 894 (2002).
168. K. Izutsu, S. Kojima. *J. Pharm. Pharmacol.* **54**, 1033 (2002).
169. K. Izutsu, S. O. Ocheda, N. Aoyagi, S. Kojima. *Int. J. Pharm.* **273**, 85 (2004).
170. M. F. Mazzobre, M. P. Buera. *Biochim. Biophys. Acta* **1473**, 337 (1999).
171. B. Wunderlich. In *Thermal Characterization of Polymeric Materials*, E. A. Turi (Ed.), pp. 91–234, Academic Press, New York (1981).

172. L. H. Sperling. In *Introduction to Physical Polymer Science*, 2nd ed., p. 594, John Wiley, New York (1992).
173. Y. H. Roos. *J. Therm. Anal. Calorim.* **71**, 197 (2002).
174. J. L. Green, J. Fan, C. A. Angell. *J. Phys. Chem.* **98**, 13780 (1994).
175. M. S. Rahman, S. Kasapis, N. S. Z. Al-Kharusi, I. M. Al-Marhubi, A. J. Khan. *J. Food Eng.* **80**, 1 (2007).
176. S. B. Matiacevich, M. L. Castellión, S. B. Maldonado, M. P. Buera. *Thermochim. Acta* **448**, 117 (2006).
177. C. G. Biliaderis, C. M. Page, T. J. Maurice, B. O. Juliano. *J. Agric. Food Chem.* **34**, 6 (1986).
178. K. J. Zeleznak, R. C. Hoseney. *Cereal Chem.* **64**, 121 (1987).
179. T. J. Laaksonen, Y. H. Roos. *J. Cereal Sci.* **33**, 331 (2001).
180. T. J. Laaksonen, Y. H. Roos. *J. Cereal Sci.* **37**, 319 (2003).
181. S. J. Schmidt. *Adv. Food Nutr. Res.* **48**, 1 (2004).
182. E. Vittadini, L. C. Dickinson, P. Chinachoti. *Carbohydr. Polym.* **46**, 49 (2001).
183. X. Lin, R. Ruan, P. Chen, M. Chung, X. Ye, T. Yang, C. Doona, T. Wagner. *J. Food Sci.* **71**, R136 (2006).
184. A. Farahnaky, I. A. Farhat, J. R. Mitchell, S. E. Hill. *Food Hydrocol.* **23**, 1483 (2009).
185. P. S. Belton, I. J. Colquhoun, J. M. Field, A. Grant, P. R. Shewry, A. S. Tatham. *J. Cereal Sci.* **19**, 115 (1994).
186. A. E. Farroni, S. B. Matiacevich, S. Guerrero, S. M. Alzamora, M. P. Buera. *J Agric. Food Chem.* **56**, 6447 (2008).
187. H.-D. Isengard, T. P. Labuza, P. J. Lillford, D. S. Reid. *IUFoST Bull.* <http://www.iufost.org/reports_resources/bulletins/IUF.SIB.Waterinfood.pdf.pdf> August (2008).
188. M. Sugisaki, H. Suga, S. Seki. *Bull. Chem. Soc. Jpn.* **41**, 2591 (1968).
189. V. Velikov, S. Borik, C. A. Angell. *Science* **294**, 2335 (2001).
190. V. R. N. Telis, P. J. Sobral. *Lebensm.-Wiss. Technol.* **34**, 199 (2001).
191. D. P. Miller, J. J. de Pablo, H. R. Corti. *J. Phys. Chem. B* **103**, 10243 (1999).
192. S. Suzuki, S. Kitamura. *Food Hydrocol.* **22**, 862 (2008).
193. J. Liesebach, T. Rades, M. Lim. *Thermochim. Acta* **401**, 159 (2003).
194. C. A. Angell, D. R. Bressel, J. L Green, H. Kanno, M. Oguni, E. J. Sare. *J. Food Eng.* **22**, 115 (1994).
195. J. M. V. Blanshard, P. J. Lillford. In *The Glassy State in Foods*, Nottingham University Press, Loughborough, UK (1993).
196. R. Parker, S. G. Ring. *Cryo-Lett.* **16**, 197 (1995).
197. W. L. Kerr, D. S. Reid. *Lebensm.-Wiss. Technol.* **27**, 225 (1994).
198. Y. I. Matveev, V. Y. Grinberg, V. B. Tolstoguzov. *Food Hydrocol.* **14**, 425 (2000).
199. Z. Qiu, J. G. Stowell, K. R. Morris, S. R. Byrn, R. Pinal. *Int. J. Pharm.* **303**, 20 (2005).
200. R. M. Hill, L. A. Dissado. *J. Phys. C: Solid State Physics* **15**, 5171 (1982).
201. O. R. Fennema, S. Damodaran, D. S. Reid. In *Fennema's Food Chemistry*, S. Damodaran, K. L. Parkin, O. R. Fennema (Eds.), pp. 17–82, CRC Press, Boca Raton (2008).
202. M. Peleg. *Crit. Rev. Food Sci. Nutr.* **32**, 59 (1992).
203. K. A. Nelson, T. P. Labuza. *J. Food Eng.* **22**, 271 (1994).
204. M. P. Longinotti, H. R. Corti. *J. Phys. Chem. Ref. Data* **37**, 11503 (2008).
205. L. Manzocco, M. C. Nicoli, M. Anese, A. Pitotti, E. Maltini. *Food Res. Int.* **31**, 363 (1998).
206. M. P. Recondo, B. E. Elizalde, M. P. Buera. *J. Food Eng.* **77**, 126 (2006).
207. H. A. Islesias, J. Chirife. *J. Food Technol.* **13**, 137 (1978).
208. S. J. Schmidt, H. Lai. In *Water Relationships in Foods*, H. Levine, L. Slade (Eds.), pp. 405–452, Plenum Press, New York (1991).
209. K. Jouppila, Y. H. Roos. *Carbohydr. Polym.* **32**, 95 (1997).

210. K. Jouppila, J. Kansikas, Y. H. Roos. *Biotechnol. Prog.* **14**, 347 (1998).
211. C. J. Kedward, W. Macnaughtan, J. R. Mitchell. *J. Food Sci.* **65**, 324 (2000).
212. R. D. L. Marsh, J. M. V. Blanshard. *Carbohydr. Polym.* **9**, 301 (1988).
213. E. A. M. Omar, Y. H. Roos. *Lebensm.-Wiss. Technol.* **40**, 536 (2007).
214. K. Jouppila, J. Kansikas, Y. H. Roos. *Carbohydr. Polym.* **36**, 143 (1998).
215. M. Avrami. *J. Chem. Phys.* **7**, 1103 (1939).
216. A. N. Kolmogorov. *Bull. Acad. Sci. USSR (Sci. Mater. Nat.)* **3**, 3551 (1937).
217. W. A. Johnson, R. F. Mehl. *Trans. AIME* **135**, 416 (1939).
218. P. L. Russell. *Starch/Staerke* **35**, 277 (1983).
219. M. A. Del Nobile, T. Martoriello, G. Mocci, E. La Notte. *J. Food Eng.* **59**, 123 (2003).
220. P. Chinachoti. In *The Properties of Water in Foods, ISOPOW 6*, D. S. Reid (Ed.), Blackie Academic, London (1998).
221. Y. Kou, L. C. Dickinson, P. Chinachoti. *J. Agric. Food Chem.* **48**, 5489 (2000).
222. P. Chatakanonda, P. Chinachoti, K. Sriroth, K. Piyachomkwan, S. Chotineeranat, H. R. Tang, B. Hills. *Carbohydr. Polym.* **53**, 233 (2003).
223. S. Ablett, A. H. Darke, M. J. Izzard, P. J. Lillford. In *The Glassy State in Foods*, J. M. V. Blanshard, P. J. Lillford (Eds.), pp. 189–206, Nottingham University Press, Loughborough, UK (1993).
224. R. Partanen, V. Marie, W. MacNaughtan, P. Forssell, I. Farhat. *Carbohydr. Polym.* **56**, 147 (2004).
225. M. Watanabe, T. Kikawada, N. Minagawa, F. Yukuhiro, T. Okuda. *J. Exper. Biol.* **205**, 2799 (2002).
226. J. M. Aguilera, M. Karel. *Crit. Rev. Food Sci. Nutr.* **37**, 287 (1997).
227. J. Buitink, O. Leprince. *Cryobiology* **48**, 215 (2004).
228. F. A. Hoekstra. *Integr. Comp. Biol.* **45**, 725 (2005).
229. R. L. Obendorf. *Seed Sci. Res.* **7**, 63 (1997).
230. U. M. N. Murthy, P. P. Kumar, W. Q. Sun. *J. Exp. Bot.* **54**, 1057 (2003).
231. P. Cerrutti, M. Segovia, M. Galvagno, C. Schebor, M. P. Buera. *Appl. Microbiol. Biotechnol.* **54**, 575 (2000).
232. C. Walters. *Biophys. J.* **86**, 1253 (2004).
233. V. Panza, V. Láinez, S. B. Maldonado, H. Maroder, M. P. Buera. In *Water Properties of Food, Pharmaceutical and Biological Materials*, M. P. Buera, J. Welti-Chanes, P. Lillford, H. R. Corti (Eds.), CRC Taylor and Francis, Boca Raton (2006).
234. M. Sacandé, J. Buitink, F. A. Hoekstra. *J. Exp. Bot.* **51**, 635 (2000).
235. M. S. Clark, M. A. S. Thorne, J. Purać, G. Grubor-Lajšić, M. Kube, R. Reinhardt, M. R. Worland. *BMC Genomics* **8**, 475 (2007).
236. H. Kawahara. *J. Biosci. Bioeng.* **94**, 492 (2002).
237. K. E. Zachariassen, E. Kristiansen. *Cryobiology* **41**, 257 (2000).
238. B. Li, D.-W. Sun. *J. Food Eng.* **54**, 175 (2002).
239. M. Harding, P. Anderberg, A. D. J. Haymet. *Eur. J. Biochem./FEBS* **270**, 1381 (2003).
240. S. R. Payne, D. Stanford, A. Harris, O. A. Young. *Meat Sci.* **37**, 429 (1994).
241. J. Li, T.-C. Lee. *Trends Food Sci. Technol.* **6**, 259 (1995).
242. M. Watanabe, S. Arai. *J. Food Eng.* **22,** 453 (1994).
243. L. Zhang, W. Zhu, L. Song, Y. Wang, H. Jiang, S. Xian, Y. Ren. *Int. J. Mol. Sci.* **10**, 2031 (2009).
244. A. F. Heneghan, P. W. Wilson, A. D. J. Haymet. *Proc. Natl. Acad. Sci. USA* **99**, 9631 (2002).
245. E. Gabellieri, G. B. Strambini. *Biophys. J.* **90**, 3239 (2006).
246. D. Mietchen, D. Manz, F. Volke, K. Storey. *PLoS ONE* **3**, 1 (2008).
247. M. S. Rahman. *Trends Food Sci. Technol.* **17**, 129 (2006).
248. S. S. Sablani, S. Kasapis, M. S. Rahman. *J. Food Eng.* **78**, 266 (2007).
249. N. Murase, F. Franks. *Biophys. Chem.* **34**, 293 (1989).
250. B. S. Chang, C. S. Randall. *Cryobiology* **29**, 632 (1992).

251. O. R. Fennema. In *Low-temperature Preservation of Foods and Living Matter*, O. R. Fennema, W. D. Powrie, E. H. Marth (Eds.), pp. 101–149, Marcel Dekker, New York (1973).
252. M. M. Sá, A. M. Sereno. *Thermochim. Acta* **246**, 285 (1994).
253. M. S. Rahman, S. Sablani, N. Al-Habsi, S. Al-Maskri, R. Al-Belusi. *J. Food Sci.* **70**, E135 (2005).
254. A. M. Goula, T. D. Karapantsios, D. S. Achilias, K. G. Adamopoulos. *J. Food Eng.* **85**, 73 (2008).
255. S. Kasapis, M. S. Rahman, N. Guizani, M. Al-Aamri. *Agric. Food Chem.* **48**, 3779 (2000).
256. Y. Bai, M. S. Rahman, C. O. Perera, B. Smith, L. D. Melton. *Food Res. Int.* **34**, 89 (2001).
257. J. Welti-Chanes, J. A. Guerrero, M. E. Barcenas, J. M. Aguilera, F. Vergara, G. V. Barbosa-Canovas. *J. Food Process. Eng.* **22**, 91 (2007).
258. G. Moraga, N. Martínez-Navarrete, A. Chiralt. *J. Food Eng.* **72**, 147 (2006).
259. H. Wang, S. Zhang, G. J. Chen. *J. Food Eng.* **84**, 307 (2008).
260. P. J. A. Sobral, V. R. N. Telis, A. M. Q. B. Habitante, A. Sereno. *Thermochim. Acta* **376**, 83 (2001).
261. M. A. Silva, P. J. A. Sobral, T. G. J. Kieckbuscha. *J. Food Eng.* **77**, 426 (2006).
262. R. M. Syamaladevi, S. S. Sablani, J. Tang, J. Powers, B. G. Swanson. *J. Food Eng.* **91**, 460 (2009).
263. S. Khalloufi, Y. El-Maslouhi, C. Ratti. *J. Food Sci.* **65**, 842 (2000).
264. M. J. Fabra, P. Talens, G. Moraga, N. Martínez-Navarrete. *J. Food Eng.* **93**, 52 (2009).
265. S. S. Sablani, L. Bruno, S. Kasapis, R. M. Symaladevi. *J. Food Eng.* **90**, 110 (2009).
266. A. E. Delgado, D. Sun. *J. Food Eng.* **55**, 1 (2002).
267. M. S. Rahman, S. Kasapis, N. Guizani, O. S. Al-Amri. *J. Food Eng.* **57**, 321 (2003).
268. T. Suzuki. *Food Hydrol.* **22**, 862 (2008).
269. C. Ohkuma, K. Kawai, C. Viriyarattanasak, T. Mahawanich, S. Tantratian, R. Takai, T. Suzuki. *Food Hydrocol.* **22**, 255 (2008).
270. R. C. Brake, O. R. Fennema. *J. Food Sci.* **64**, 10 (1999).
271. K. Tanaka, T. Takeda, K. Miyajima. *Chem. Pharm. Bull.* **39**, 1091 (1991).
272. A. Ramos, N. D. H. Raven, R. J. Sharp, S. Bartolucci, M. Rossi, R. Cannio, J. Lebbink, J. Van Der Oost, W. M. De Vos, H. Santos. *Appl. Environ. Microbiol.* **83**, 4020 (1997).
273. A. Hawe, W. Friess. *Eur. J. Pharm. Sci.* **28**, 224 (2006).
274. N. K. Jain, I. Roy. *Eur. J. Pharm. Biopharm.* **69**, 824 (2008).
275. S. D. Allison, A. Donga, J. F. Carpenter. *Biophys. J.* **71**, 2022 (1996).
276. L. Bush, C. Webb, L. Bartlett, B. Burnett. *Semin. Hematol.* **35**, 18 (1998).
277. W. Garzon-Rodriguez, R. L. Koval, S. Chongprasert, S. Krishnan, T. W. Randolph, N. W. Warne, J. F. Carpenter. *J. Pharm. Sci.* **93**, 684 (2003).
278. B. S. Chang, G. Reeder, J. F. Carpenter. *Pharm.* **13**, 243 (1996).
279. Y. Han, B. S. Jin, S. B. Lee, Y. Sohn, J. Joung, J. H. Lee. *Arch. Pharm. Res.* **30**, 1124 (2007).
280. S. J. Prestrelski, T. Arakawa, J. F. Carpenter. *Arch. Biochem. Biophys.* **303**, 465 (1993).
281. A. W. Ford, P. J. Dawson. *J. Pharm. Pharmacol.* **45**, 86 (1993).
282. S. B. Petersen, V. Jonson, P. Fojan, R. Wimmer, S. Pedersen. *J. Biotechnol.* **114**, 269 (2004).
283. F. W. L. Hulse, R. T. Forbes, M. C. Bonnera, M. Getrost. *Eur. J. Pharm. Sci.* **33**, 294 (2008).
284. R. A. DePaz, D. A. Dale, C. C. Barnett, J. F. Carpenter, A. L. Gaertnerb, T. W. Randolph. *Enzyme Microb. Technol.* **31**, 765 (2002).
285. M. S. Rahman. *Int. J. Food Properties* **7**, 407 (2004).
286. M. S. Rahman, R. M. Al-Belushi, N. Guizani, G. S. Al-Saidi, B. Soussi. *Food Chem.* **114**, 1257 (2009).